Environmental changes and the rise and fall of civilizations in the northern Horn of Africa: an approach combining δD analyses of land-plant derived fatty acids with multiple proxies in soil

Valery T. Terwilliger, Zewdu Eshetu, Jean-Robert Disnar, Jérémy Jacob, Paul W. Adderley, Yongsong Huang, Marcelo Alexandre, Marylin L. Fogel

Environmental changes and the rise and fall of civilizations in the northern Horn of Africa: an approach combining δD analyses of land-plant derived fatty acids with multiple proxies in soil.

Valery J. Terwilliger[a,b,c,*], Zewdu Eshetu[d], Jean-Robert Disnar[b], Jérémy Jacob[b], W. Paul Adderley[e], Yongsong Huang[f], Marcelo Alexandre[g], Marilyn L. Fogel[h]

[a] University of Kansas, Department of Geography, Lawrence, KS, USA

[b] Institut des Sciences de la Terre d'Orléans (ISTO), Université d'Orléans, UMR 7327 du CNRS/INSU, Orléans, France

[c]LE STUDIUM®, Loire Valley Institute for Advanced Studies, Orléans, France

[d] University of Addis Ababa, Department of Paleoanthropology and Paleoenvironment, Addis Ababa, Ethiopia

[e] University of Stirling, Biological and Environmental Sciences, School of Natural Sciences, Stirling, Scotland, UK

[f] Brown University, Department of Geological Sciences, Providence, RI, USA

[g] Universidade Federal de Sergipe, Departamento de Química, São Cristóvão, Brasil

[h] Carnegie Institution of Washington, Geophysical Laboratory, Washington, DC, USA

* Corresponding author. Tel.: +1 785 864 5143
E-mail address: terwilli@ku.edu

Submit to: Geochimica et Cosmochimica Acta

Key words: stable isotopes, δD *n*-alkanoic acids, soil image-analysis, Rock-eval pyrolysis, paleoenvironmental reconstruction, soil organic matter, Ethiopian Plateau

Abstract

The domains of the ancient polities D'MT and Aksum in the Horn of Africa's highlands are a superior natural system for evaluating roles of environmental change on the rise and fall of civilizations. To compare environmental changes of the times of the two polities, we analyzed stable hydrogen isotopic ratios (δD) of land-plant derived fatty acids (*n*-$C_{26–30}$) and other proxies from soil sequences spanning the Holocene from the region. Three results suggest that trends in δD values unambiguously reflect changes in rainfall. First, increases in δD coincide with dry periods inferred from studies of eastern African lakes. Second, changes in δD values were parallel among sections during overlapping time intervals. Third, consideration of vegetation history did not alter directions of trends in δD values over time. By unambiguously recording precipitation, the δD values also enhanced interpretations of proxies that are affected by both climate and land clearing.

Both D'MT (ca 2750–2350 cal y BP) and the Aksumite (ca 2100–1250 cal y BP) rose during wetter intervals of the drier part of the Holocene (after ca 6000 cal y BP). Analyses of charred matter indicated that fire had been a common agent of land clearing in all sites. The influence of climate on fire varied, however. Prior to the emergence of D'MT, δD values were correlated with C_4:C_3 plant ratios estimated from $\delta^{13}C$ values. There are no C_4 trees and precipitation may have been the main influence on canopy openness. After ca 4300 cal y BP, there was no significant relationship between δD and C_4:C_3 plant ratios suggesting that factors such as fire influenced canopy openness regardless of climate. Furthermore, the impact of land clearance differed between sites and between D'MT and the Aksumite's times. In one site, the interval from 3550 cal y BP to the decline of D'MT had several anomalies that suggested dramatic increases in thermal severity of fire and human impact. Among these were a large contribution of charred matter to a high % total organic carbon that low hydrogen and oxygen indices suggest was severely altered by other factors than humification. These results support hypotheses about the rise of civilizations being favored by specific climatic conditions but suggest that patterns of land clearing differed during the declines of D'MT and the Aksumite.

1. INTRODUCTION

Environmental changes have been linked to as widely ranging factors shaping the complexity of civilizations as food security and attitudes about non-conformity (Diamond, 2005; Büntgen et al., 2011; Gelfand et al., 2011). Research to understand the nature of links between past environments and the rise and fall of civilizations is sought for managing consequences of present global environmental changes (CCSP, 2003; IPCC, 2007; Mastrandea and Schneider, 2010). Paleoenvironmental records have been a key component of such research (Aimers, 2011).

Needs for progress are now recognized in two applications of paleoenvironmental records to evaluate effects of environment on cultural complexity. One need is better local-scale environmental records (Dergachev et al., 2007; Emery and Thornton, 2008; Giorgi et al., 2008; Jones et al., 2009; Hodell, 2011). This is a prerequisite to the larger need to understand if certain environmental changes have predictable consequences for the status of civilizations (Turchin, 2008; Beck et al., 2010). Consequences of environmental changes for civilizations have largely been deduced by linking climate records to land clearing characteristics and then to historical developments in a single polity (e.g. McGovern, 1994; deMenocal, 2001; Weiss and Bradley, 2001; Haug et al., 2003; Adderley and Simpson, 2006; Patterson et al., 2010). A strategy to understand whether environmental changes have predictable consequences for civilizations is to study locations where more than one complex polity has risen and fallen (Gebru et al., 2009; Terwilliger et al., 2011).

The Tigray Plateau of the northern Horn of Africa (hereinafter called the Plateau) has prime attributes for contributing to both of the aforementioned needs. Mountainous relief, location along the northern oscillations of the Inter-Tropical Convergence Zone, and proximity to an active triple junction of plate tectonic activity assure large spatial and temporal changes in environment. The Plateau's networks of gullies expose soil sequences that have rich archives of proxies for local-scale environmental changes during continuous time intervals throughout the Holocene (Berakhi et al., 1998; Machado, 1998; Dramis et al., 2003; Gebru et al., 2009; Terwilliger et al., 2011). The succession of complex polities that

existed there during the Holocene make the Plateau a superior natural laboratory for examining whether environment predictably affects the status of societies. Among these was one of the major ancient civilizations of the world -- the Aksumite Empire (Duiker and Spielvogel, 2010). D'MT, which preceded Aksum, had a similar suite of the accoutrements of a civilization (Fattovich 1990, 2000, 2009; Robin and de Maigret, 1998; Bard et al., 2000).

Regardless of its importance, few studies of environmental history have been carried out on the Plateau (French, 2009; Sulas, 2010). Although likely including environmental effects, the reasons for the rise and fall of the Aksumite Empire are the least known of the major ancient civilizations (Butzer, 1981; Ehret, 2002; Connah, 2004). Whether environmental factors played similar roles on the emergence and disintegration of both D'MT and Aksum is unknown. The few paleoenvironmental records of the Plateau are largely derived from classical analyses of soil geomorphology. Conclusions about precipitation and land clearing patterns vary markedly among these studies (reviewed in Nyssen et al., 2004). Because precipitation or land clearing may have similar impacts on physical landscapes, these differences in interpretation may be irreconcilable using those methods alone (Butzer, 2005).

Records from an unambiguous proxy for precipitation can be used to more clearly interpret proxies affected by climate and land clearing (Gebru et al., 2009; Terwilliger et al., 2008, 2011). Stable hydrogen isotopic analyses of land-plant derived lipid compounds extracted from soils and aquatic sediments are promising sources of information about paleohydrology (Sachse et al., 2012). The original source of hydrogen for lipid synthesis is water used in photosynthesis and the basis for the climate signal in the lipid is the influence of climate on the δD of that water (Dansgaard, 1964; Sternberg, 1989). Exactly how variable that influence is among plant types and how constant the hydrogen fractionation is from source water to specific lipid synthesis remain active areas of research, however, with implications meriting consideration in paleoclimate interpretation (e.g., Sachse et al., 2004, 2006; Hou et al., 2008; Feakins and Sessions, 2010a; Garcin et al., 2012).

The main objective of this paper is to examine whether environments within the two

most complex of the Plateau's ancient polities; D'MT (ca 2750–2350 cal y BP) and the Aksumite Empire (ca 2100–1250 cal y BP), were similar at similar stages of development. This is a contribution to addressing the question "do certain environmental changes have predictable consequences for the rise and fall of civilizations?" For this purpose, we built records of local-scale climate and land clearing changes from proxies in exposed soil sequences at several sites that were within the domains of both D'MT and Aksum. These include analyses of δD values of land-plant derived saturated fatty acid compounds, $\delta^{13}C$ of bulk organic matter, fire-related soil micro-imagery, elements (of P and organic C), and organic matter quality (Rock-Eval pyrolysis). This study is distinctive in its use of paleoprecipitation records from molecular level δD analyses to reduce ambiguities in inferences about land clearing from other proxies.

2. SAMPLING SITES AND STRATEGY

2.1. Site locations, environments, and history

The Plateau was the site of a long, rich history of human groups that were at least as complex as kingdoms. Indications are that D'MT and Aksum were the most complex of these, attaining the accoutrements associated with many definitions of a civilization. These included novel writing systems, an urban center, international trade, agricultural innovation, a hinterland of agricultural communities, metallurgy, plow agriculture, water management technologies, and monumental stone architecture (DiBlasi, 2005; Fattovich, 2009). This paper particularly concerns itself with the environments during the times of the rise and fall of D'MT (ca 2750–2350 cal y BP) and of Aksum (ca 2100–1250 cal y BP) but see Gebru et al. (2009) for a more comprehensive summary timeline of developments in major polities of the Plateau .

We selected three sites with gullies exposing soil profiles in an Ethiopian portion of the Plateau that was first in D'MT and later in the Aksumite Empire (Fig. 1). We use the word "soil" in this paper to refer to unconsolidated deposits that are not under water, regardless of whether horizon development has occurred. Sites were chosen in the hinterlands of the

civilizations. Named after their nearest towns, they are Adi Kolan (AK, 2171 m a. s. l.), Mai Maikden (MM, 2228 m a. s. l.), and Adigrat (AT, 2493 m a. s. l.). Although none is a known archeological settlement site, their physical characteristics and proximity to known ancient settlements suggest long agricultural histories (Phillipson, 1998; D'Andrea et al., 2008; 2011; Curtis, 2009).

The sites have similar rainfall distributions but temperature decreases and rainfall increases slightly from the lowest (AK, 563 mm y^{-1}) to the highest (AT, 619 mm y^{-1}) elevations (National Meteorological Agency of Ethiopia, 1998–2006). The watersheds of all three sites have nearly identical plant cover consisting mostly of heavily grazed *Acacia* spp. dominated grassland and fit the description of floodplain as they are flat and surrounded by mountains (Fig. 1). This vegetation is highly altered by human activity. The natural vegetation is unknown but is thought to be Afromontane (Friis, 1992). Sources of non-aeolian contributions to their soils are unlikely to be more than 10 km distant at either AT or MM, and 20 km at AK. In general, the mantle of soil of the Plateau overtops Tertiary basalts associated with volcanism of the East African Rift. Further detail about lithology is provided in Gani et al., (2007), Gebru et al. (2009), and Terwilliger et al. (2011).

2.2. Study section descriptions and sampling protocols

One soil section per site was sampled for the full suite of proxies reported in this paper: AKIII (13° 19' 55.80" N, 39° 21' 52.56" E); MMII (13°35'1.05"N, 39°34'4.64"E); and ATI 14° 16' 13.56" N, 39° 26' 52.18" E). AKIII and ATI are mineral soils distributed in layers of widely ranging textures and structures (Fig. 2, Appendix A). MMII is mostly older than 4500 cal y BP reworked travertine and peat overtopped by very young mineral soil. Each section was excavated at least 1 m back from its wall. Sampling intervals were 10 cm or less for analyses of $\delta^{13}C$ and percent total organic carbon of bulk organic matter. Compound specific isotopic, Rock-Eval pyrolysis, micromorphological, and total phosphorus analyses were made on selected samples of this collection. Selection criteria included even representation of time intervals followed by targeting of samples representing changes in soil morphology.

A separate sample set was obtained for radiocarbon dating, identification of charcoalized wood fragments, and descriptive analyses of soil characteristics such as texture, pH, and electrical conductivity. Protocols for soil sampling, drying, and storage prior to analyses are described further in Gebru et al. (2009) and Terwilliger et al. (2011).

3. METHODS

3.1. Land-plant derived fatty acid δD analyses

We analyzed δD values of long-chain (> *n*-C24) *n*-alkanoic (fatty) acids in this study because they were consistently more abundant than other *n*-alkyl lipid groups -- *n*-alkanes and *n*-alkanols -- that largely have land-plant sources (Eglinton and Hamilton, 1967; Kolattukudy, 1970). Extractions for analyses of δD values of specific, land-plant derived saturated fatty acids followed methods used in Huang et al. (2004). Specifically, total lipids were extracted from ca 12 g of soil per sample with 9:1 dichloromethane (DCM) and methanol (MeOH) at high temperature (120 ^{o}C) and pressure (1200 psi) using an accelerator solvent extractor (ASE 200, Dionex). Solid phase extraction columns (either Pasteur pipettes packed with aminopropyl or Supelclean™ LC-NH_2 SPE tubes) were used for elution of first, the neutral fraction (with DCM and isopropanol) and next, the fatty acids (with ether and acetic acid). Fatty acids were then dissolved in toluene, derivatized by methylation with MeOH of known δD acidified with acetyl chloride, and heated in closed vials at 60^{o}C for 12 h. NaCl solution was then added to the methylated sample followed by liquid-liquid extraction using hexane. Fatty acid methyl esters (FAMEs) were further purified through a silica gel column by first removing contaminants with hexane and then eluting the FAMEs with DCM.

FAME δD values were analyzed by gas chromatography stable isotope mass spectrometry (GC-IRMS) that recognized compounds from the retention times of their peaks. FAME δD values of most AKIII and all of the MMII samples were obtained at Brown University by a GC (Agilent 6890) coupled to an IRMS (Finnigan Delta-plus XL) via a combustion module (Finnigan GC Combustion III). Concentrations were determined by Gas Chromatography-Flame Ionization Detection (GC-FID). The FAME δD values of samples

from ATI as well as some duplicate and additional samples from AKIII were obtained at Carnegie Institution on a GC (TRACE, ThermoFisher) coupled to an IRMS (Delta-plusXL, Thermo Finnigan) with a GC Combustion III interface. An HP1MS 30 m x 0.32 mm x 0.25 µm column was used at Brown University; a 60 m column at Carnegie Institution. In both GC-IRMS systems, samples were injected in pulsed splitless mode at 20 PSI for 1 min at a temperature of 320^{o}C at Brown University and at 300^{o}C at Carnegie Institution. Otherwise, GC running conditions were identical for the two systems.

An external standard with 6 peaks (*n*-C_{16}, *n*-C_{18}, *n*-C_{22}, *n*-C_{24}, *n*-C_{26}, and *n*-C_{28}), calibrated against a certified standard often used in Huang's lab was used on both the Brown University and Carnegie Institution GC-IRMS systems. The standard errors in δD values were < 2.0 in each system. FAME δD values (δD_{FAME}) were converted to δD values of their source compounds (δD C_S) by correcting for the 3 Hs from methylation (δD_{MeOH}) via the mass balance approximation

$$\delta D\ C_S = [\delta D_{FAME} - (3/n\ \delta D_{MeOH})]/[(n-3)/n] \quad \textbf{[1]}$$

where n denotes the number of hydrogen atoms in the specific source fatty acid. Mean δD values of compounds in the standard differed by < 2.5‰ between laboratories, which was not statistically significant (t test, $p \geq 0.2$).

3.2. Soil micromorphology and phosphorus contents

Thin sections were cut from 64 intact soil peds from AKIII, MMII, and ATI to obtain quantitative microscopic image data about charred organic matter that are relevant to land clearing by fire. The samples were vapor-phase dried with acetone, then vacuum impregnated with polyester resin (Crystic 17449, Scott Bader PLC) according to standard methods at the University of Stirling (www.thin.stir.ac.uk). The resulting block was mounted, and sections cut, ground, and polished to 30 µm thickness (as per Murphy, 1984; Adderley et al., 2002). Representative portions of each section were then selected by optical microscopy at x40–x200 magnification. Using different illumination methods, four sets of images were obtained from each portion via a polarized optical microscope, CCD camera, and imaging

software (AnalySIS, Olympus Optical Co.) at x80 magnification. These were: 1) transmitted plane polarized (ppl), 2) crossed-polarizers at 45^{o} and 90^{o} (xpl), 3) circularly polarized (cpl), and 4) reflected oblique incident illumination (oil).

Images were segmented using color and morphological criteria to distinguish charred organic matter (Adderley et al., 2002, 2010). First, pore space was identified by matching and comparing segments from the aforementioned cpl and xpl images; a process that eliminates the potential for mistaking basal-cut quartz grains for pores from the cpl images alone (Whalley et al., 2005). The methods of Simpson et al. (2003) were then extended to distinguish charred from other darkened materials, including peat, for the extremely wide range of soil colors and textures among our samples (Terwilliger et al., 2011). Our modification consisted of determining thresholds for charcoal-derived *vs* other organic materials by matching ppl and oil images and performing a set of pixel-level Boolean operations to distinguish the color (via ppl) and texture (oil) of charred from other dark materials. The total area attributable charred matter in each object was then recorded.

Total phosphorus content was analyzed to provide insights about anthropogenic impacts on landscapes on 10 g of ground soil from all samples that also provided peds for image analyses. These soils underwent acid-perfusate digestion followed by inductively coupled plasma- atomic emission spectroscopy (ICP-AES; Perkin Elmer Optima 5300DV) analyses (as per Association of Official Agricultural Chemists, 2000).

3.3. Organic matter quality

The state of preservation of organic matter was assessed from hydrogen (HI) and oxygen indices (OI) by Rock-Eval pyrolysis on an RE6 (Vinci Technologies)(rationales in Espitalié et al., 1985a; b; Disnar et al., 2003, 2008). HI is the mass of hydrocarbon-rich substances that is released during the pyrolysis phase of instrument operation, per mass of total organic carbon (TOC). OI is a measure of the oxygen content of the organic matter as given by the mass of O_2 in $CO + CO_2$ released during pyrolysis per mass TOC.

3.4. Bulk C isotopic and elemental analyses, charcoal ^{14}C dating and identification

Most bulk isotopic, carbon elemental, radiocarbon date and forest history data in this study have been published for other contexts. Further detail than that below about how they were obtained and analyzed are in Gebru et al. (2009) and Terwilliger et al. (2011).

Percent total organic carbon (%TOC) and $\delta^{13}C$ values were obtained with an elemental analyzer (Carlo Erba NA 1500) coupled via continuous flow to a stable isotope ratio mass spectrometer (Conflo II to Delta XL plus, ThermoFinnigan). The δ notation for the stable isotopic composition of each element (X) is defined by the equation

$$\delta X = [(R_{sample}/R_{standard)} - 1] \, 1000 \; (‰) \qquad \textbf{[2]}$$

where $R = [^hX/^lX]$, h = heavier isotope, l = lighter isotope, and the standard is Pee Dee Belemnite (Craig, 1957). The precision of the measurements was better than ± 0.2‰.

The percentage of all (C_3 + C_4) carbon from C_4 plants in SOM ($\%C_4$) was estimated using the equation (Trouve et al., 1994)

$$\%C_4 = 100 \, (\delta^{13}C_{SOM} - \delta^{13}C_{C3})/(\delta^{13}C_{C4} - \delta^{13}C_{C3}) \qquad \textbf{[3]}$$

The value used for $\delta^{13}C_{C3}$ was -29.09‰ and -12.79‰ for $\delta^{13}C_{C4}$. These $\delta^{13}C$ values were averages obtained from C_3 and C_4 plants collected at Debre-Zeit and Kulumsa agricultural experimental stations at similar elevation ranges to those of the study sites. The $\%C_4$ values reported herein have no further corrections. Nonetheless, we considered and, where possible, modeled effects of a variety of factors other than photosynthetic pathway of plant sources that may influence $\delta^{13}C_{SOM}$ values. These included Suess effect, decomposition, soil texture, and the correction that it would take to change a conclusion that C_4 plants had dominated to an interpretation that >50% of the vegetation had been C_3 (details in Terwilliger et al., 2011). If all of these factors are considered, %C4 estimates from [3] may be overestimated in all samples older than 150 cal y BP but the directions of changes in %C4 are likely robust.

Where present, charcoalized wood was obtained from soil samples by bucket flotation methods. Where possible, fragments were identified. This paper shows changes in relative compositions of gymnosperm (*Juniperus procera* forest communities) and angiosperm

253 (secondary forest or *Acacia* spp. woodland) trees. Charcoal was dated at the University of
254 California at Irvine's Keck Carbon Cycle Accelerator Mass Spectrometry facility (Table 1).
255 Radiocarbon ages were converted to calendar years before present (cal y BP, 1950 CE =
256 present) using CALIB v5.0.2 (Stuiver and Reimer, 1986-2005) software and considerations in
257 Stuiver and Reimer (1993). The median of the probability distribution for the calibration
258 curve was used as a single estimate for the calendar age of a sample and was obtained from
259 the aforementioned software. The median and the weighted average of the probability
260 distribution of calibrated ages are the more robust of present single values for describing
261 calendar age (Telford et al., 2004). Age-depth relationships for each section were
262 determined by linear interpolation between charcoal dates with modifications suggested by
263 changes in soil morphology.
264
265 **3.5. Soil physical and salinity description**
266 Additional analyses of soil physical characteristics informed sampling protocols,
267 calculations of chronologies, and possible influences of sality. These included field
268 observations of changes in color, grain size, structure grade, and dry consistence using
269 Munsell Soil Color Charts (1994) and guidelines in Schoeneberger et al. (2002). Soil texture
270 was analyzed by a combination of dry sieving and the Bouyoucos (1936) hydrometer method
271 with texture names following the United States Department of Agriculture classification (Soil
272 Survey Staff, 1995). Soil pH and Electrical Conductivity (EC) were measured to assess
273 salinity where soils with pH < 8.5 and EC > 4 were defined as saline where pH was
274 measured by a potentiometer on soil suspended in water and EC water determined by the
275 water saturated soil paste method (Rhoades, 1993). All texture, pH, and EC analyses were
276 made by the Ethiopian National Soil Research Laboratory.
277
278 **3.6. Statistical analyses**
279 Data were examined for simple long-term trends over time with a maximum of one
280 shift (optimal breakpoint) in those trends dividing a section into a maximum of two trend

segments using segmented line regression analyses (Draper and Smith, 1981; Thomson, 1990). The optimal breakpoint for a shift was the point within the range of significant breakpoints with the largest coefficient of explanation (Oosterbaan et al., 1990). To cross-check or discretely discern environmental inferences, data from different pairs of proxies were examined for co-variation using correlation analysis that tested the Pearson's product-moment correlation coefficient for significance (Sokal and Rohlf, 1995).

Segmented regression analyses were performed using SegReg (Oosterbaan, no date). All other statistical analyses were performed using Minitab (version 13, State College, PA, USA). All statistical tests were considered to be significant at $p \leq 0.05$.

4. RESULTS

4.1. Lithology, chronology, and salinity

Together, the three sections spanned the last 8300 years and also represented a short time interval before ca 13,700 cal y BP (Table 1, Fig. 2). Dates were predominantly well-ordered. Soil layers varied markedly in texture and structure (Fig. 2, Appendix A) within sequences; facilitating the detection of hiati in time and changes in rates of net sedimentation for calculating time sequences. No hiatus in time was detected for ATI whereas AKIII and MMII each had one hiatus. If pedogenesis had occurred in any of the sections, however, it was very weak. Charcoal fragments were distributed regularly throughout the AKIII and ATI sections although the fragments were generally smaller and more fragile in AKIII. The deeper portion of the travertine/peat (ca 300–640 cm) and upper mineral layers of MMII contained abundant, large fragments of charcoalized wood but charcoalized wood fragments were not found in the upper (ca 100–300 cm) of this material (Fig. 2). Detailed explanations of how soil properties and charcoal distributions were used to enhance the interpolation of chronologies for each sequence are in Gebru et al. (2009) and Terwilliger et al. (2011).

Although all but one soil sample was basic, most were normal and not saline with pH < 8.5 and EC < 4.0 dS m^{-1} (Fig. 2). Nevertheless, most of the soil from the top of the reworked travertine/peat at 100 cm to 415 cm depth in MMII was saline. This included both

the portion where we could not find charcoalized wood and some of the portion where charcoalized wood fragments were abundant.

4.2. Specific fatty acid δD and bulk organic $\delta^{13}C$ values

The δD values of the fatty acids from land plant sources (*n*-C_{26}, *n*-C_{28}, *n*-C_{30}) were significantly correlated to one another in each site (for *n*-C_{26} and *n*-C_{28} | AKIII: R=0.489, p= 0.011; MMII: R=0.861, p<0.0005; ATI: R=0.975, p<0.0005), (for *n*-C_{26} and *n*-C_{30} | AKIII: R= 0.540, p=0.004; MMII: R=0.715, p<0.0005; ATI: R=0.975, p<0.0005), (for *n*-C_{28} and *n*-C_{30} | AKIII: R=0.706, p<0.0005; MMII: R=0.851, p<0.0005; ATI: R=1, p<0.0005)(Table 2). Hereinafter, we focus only on the results for *n*-C_{26} as these consistently had the highest, most evenly-shaped peaks and the peaks were present in the most samples.

$\delta D_{n\text{-}C26}$ values ranged from -172 – -110‰ in AKIII, -217 to -126‰ in MMII, and -153 – -127‰ in ATI (Table 2). $\delta D_{n\text{-}C26}$ (but not $\delta^{13}C$) values are very similar to one another among portions of the sections that overlap in time, although values from ATI never exceed those with closely corresponding ages in the slightly more arid, lower elevation AKIII (Fig. 3). In MMII, the section with most of the older than 4500 cal y BP values, a marked (40‰) shift (optimal breakpoint) to higher $\delta D_{n\text{-}C26}$ values occurred after ca 6035 cal y BP but much earlier than the point at which older reworked travertine/peat layers end and the very recent mineral soil layer begins (Table 3, Figs. 2, 3, 4). In AKIII, which has a hiatus from ca13700–4400 cal y BP, $\delta D_{n\text{-}C26}$ values increased linearly from oldest (ca 13750 cal y BP) to youngest (present) ages (Table 3, Fig. 5). In ATI, $\delta D_{n\text{-}C26}$ shifted to higher values after ca 2440 cal y BP (Table 3, Fig.6). Furthermore, $\delta D_{n\text{-}C26}$ values decreased significantly from the oldest soil at ca 2750 until 2440 cal y BP, then switched to increase to the youngest soils (ca 500 cal y BP) of that segment.

Similar trends in $\delta^{13}C$ and $\delta D_{n\text{-}C26}$ values over time and positive correlations of $\delta^{13}C$ and $\delta D_{n\text{-}C26}$ would support the hypothesis that climate influenced changes in percentages of total organic carbon derived from C_4 plants ($\%C_4$). In MMII, $\delta D_{n\text{-}C26}$ and $\delta^{13}C$ were correlated and also shifted to higher values after the same time (6035 cal y BP)(Fig. 4; Tables 3, 4).

Where they overlapped in time, $\delta^{13}C$ values of bulk organic matter were more negative and thus $\%C_4$ was lower in ATI than in the slightly more arid AKIII (Fig. 3). Nonetheless, $\delta^{13}C$ values were not correlated with $\delta D_{n\text{-}C26}$ values in either AKIII or ATI. In contrast to $\delta D_{n\text{-}C26}$, $\delta^{13}C$ of AKIII shifted to less negative values after ca 3435 cal y BP. However, values in the time segments before and after that date either did not vary linearly with time if the sample subset paired to $\delta D_{n\text{-}C26}$ was used or increased significantly but slightly from older soils to the breakpoint, then decreased thereafter in the full data set (Fig. 5, Table 3). In ATI, the long-term trends in $\delta^{13}C$ differed not only from those in $\delta D_{n\text{-}C26}$ but also depending on whether the full or subset of data was examined (Fig. 6, Table 3). In the subset, $\delta^{13}C$ values shifted to more negative values after ca 2110 cal y BP during a time segment when $\delta D_{n\text{-}C26}$ values were increasing. In the full set, $\delta^{13}C$ values decreased from older soils until shifting to less negative values at ca 2680 cal y BP, then decreased again thereafter.

In summary, long-term linear trends emerged within the δ value sequences of each element. Large oscillations of relatively short duration occurred as well, however, regardless of whether or not there were significant long-term changes. Furthermore, although precipitation can influence the δ values of both elements, $\delta D_{n\text{-}C26}$ and $\delta^{13}C$ values are only correlated in MMII (Table 4).

4.3. Soil micromorphology, organic matter quality, elemental contents over time

4.3.1. Mai Maikden

Although shifts in values (at breakpoints) occurred in three of the five non-isotopic factors analyzed from MMII, the dates for shifts were unique to each factor (Fig. 4). Not surprisingly given its composition of peat and travertine as well as mineral soil layers (Fig. 2), percentages of organic carbon of total weight (%TOC) ranged more widely (0.4–8.5) and had larger short-term variations in MMII than in the other two sections (Table 2). Consequently the breakpoint dates for %TOC differed between tests of all available data (increase after ca 7160 cal y BP) and data from the sample subset used for comparisons with other factors (decrease after 6280 cal y BP). Furthermore, when all data were examined, %TOC

decreased from older to younger soils during both the time segments prior to and following 7160 cal y BP whereas data from the subset did not exhibit long term trends over the time segments before and after ca 6280 cal y BP. Hydrogen index values (HI) ranged from 0–163 mg HC g^{-1} TOC, decreased from older soils until ca 4915 cal y BP and then increased thereafter. Oxygen index values (OI) ranged from 236–423 mg O_2 g^{-1} TOC, decreased from the oldest soil until ca 5880 cal y BP, increased greatly at that breakpoint, and then decreased thereafter. With a range from 89–890 mg P kg^{-1}, Total phosphorus contents (Total P) were all lower in MMII than elsewhere. Total P increased from older to younger soils. In contrast, although the percent area that consisted of charred organic matter (%Char) ranged greatly from 0–68 and shifted by > 50 % over several short time intervals, there were no trends in %Char over the long term.

4.3.2. Adi Kolan

In addition to the δ values, significant shifts in three of the five non-isotopic soil analyses occurred at ca 3435 cal y BP in AKIII (Fig. 5) suggesting a simultaneous influence of environmental change at that time. %TOC, which ranged from 0.1–2.2 (Table 2), was higher after than before that date. OI decreased significantly after 3435 cal y BP and increased from older to younger soils over the time segments before and after that date. OI values ranged from 265–741 mg O_2 g^{-1}TOC. Total P also shifted from higher values before to lower values after 3435 cal y BP; decreasing from older to younger soils during the time segment prior to that date and increasing towards the present time thereafter. Total P values ranged from 1133–1976 mg P kg^{-1} in AKIII and were the highest of the three sections.

HI values in AKIII ranged from 0–80 mg HC g^{-1} TOC, decreased significantly if <1 mg HC g^{-1} TOC from the oldest soils until ca 2750 cal y BP, and then increased thereafter. The percent area that consisted of charred material (%Char) was lower after ca 2200 cal y BP than before. %Char ranged from 0.4–50 (Table 2).

4.3.3. Adigrat

Shifts in values occurred in three of the soil factors measured in ATI but the breakpoints differed among factors (Fig. 6). When all of the available data were analyzed, %TOC was significantly higher after ca 2275 cal y BP than before that date. When only the subset of values for samples matching other factors was examined, %TOC increased from older to younger soils without a breakpoint. The total range in %TOC from 0.1–1.5, was the smallest of the three sites (Table 2). HI values ranged from 0–104 mg HC g^{-1} TOC and increased from older to younger soils. OI values ranged from 375–875 mg O_2 g^{-1} TOC, and changed from a faster rate of decrease from older soils until ca 2180 cal y BP to a slower rate of decrease thereafter. Total P ranged less in value (974–1034 mg P kg^{-1}) than elsewhere and exhibited no significant long-term changes. %Char, which ranged in values from 0.9–13.8, shifted to higher values at ca 2100 cal y BP and values decreased from older to younger soils during both the time segments prior to and after that date.

4.4. Correlations between proxies

Of all possible comparisons of proxies, only two factors; OI and %TOC, were significantly correlated (negatively) with one another in all three sites (Table 4). Furthermore, factors that are commonly correlated did not co-vary in all three sites. For example, HI and OI are commonly negatively correlated with HI decreasing and OI increasing with humification (Disnar et al., 2003). Although HI and OI were negatively correlated in MMII and ATI, they were unrelated to one another in AKIII. These results suggest that each factor is discretely influenced by environment and that there were differences in the precise suite of environmental changes that occurred among sites.

5. DISCUSSION

5.1. Evaluation of δD leaf wax fatty acids as a proxy for precipitation

The source of hydrogen for any organic compound in a plant is water used in photosynthesis (Ruben et al., 1941). The original source of that water is precipitation and climate influences its δD value (Dansgaard, 1964; Yurtsever, 1975; Gat, 1980; Vimeux et al.,

1999). At tropical latitudes such as those of our sites, precipitation occurs in closest proximity to the bulk of global cloud formation and its δD values are most influenced by its amount. δD values decrease as precipitation amount increases (Risi et al., 2008). Additional factors shape the δD values of fatty acids in land-plants as well but their consideration below suggests that our $\delta D_{n\text{-}C26}$ sequences were unambiguously if qualitatively reflecting changes in amount of precipitation.

Elevation, distance from the ocean, and the fraction of global water in ice can also affect the δD values of precipitation. Any effect of distance on $\delta D_{n\text{-}C26}$ values in our study was likely constant as our sites are virtually equidistant from their oceanic source of precipitation. The tendency for $\delta D_{n\text{-}C26}$ values in ATI to be similar to but never greater than those from the overlapping time interval in AKIII may be a result of differences in elevation and/or amount of precipitation. A correction curve for the effects of changes in ice volume over the last 44,000 years on δD values of *n*-alkanes in West African marine sediments (Niedermeyer et al., 2010) suggests that differences in ice volume would only have affected the $\delta D_{n\text{-}C26}$ value of our oldest sample (ca 13,750 cal y BP at AKIII, Figs. 3, 5); lowering it by < 5‰.

Plant to plant differences in fractionations between δD values of *n*-alkyl compounds and their precipitation source may introduce the greatest error in interpreting rainfall amount. Most findings from this active area of study have been on *n*-alkanes but are probably equally applicable to fatty acids (Chikaraishi and Naraoka, 2003, 2007; Chikaraishi et al., 2004). Evaporation gradients tend to cause water to be more D-enriched at the surface of soils than at depth. As a result, differences in δD values of *n*-alkyl compounds among plant species growing in the same area may reflect differences in the depths at which their roots take up water (e.g., Krull et al., 2006). Evapotranspiration may cause the leaf water used in photosynthesis to be D-enriched compared to its precipitation source (Sternberg, 1989; Yakir, 1992), resulting in a magnification of the inverse relationship between δD values and amount of precipitation (Worden et al., 2007). Effects of evapotranspiration on δD values of leaf water may differ among plant types (Jackson et al., 1999; Smith and Freeman, 2006;

449 Feakins and Sessions, 2010a; Enquist and Enquist, 2011).

450 Hydrogen isotopic fractionations also occur during biochemical reactions leading to *n*-
451 alkyl compound synthesis. Particularly large hydrogen fractionations occur during
452 photosynthesis, metabolism, and when reactants include organic compounds that are not
453 immediate outputs from photosynthesis (photoheterotrophic or heterotrophic) (Estep and
454 Hoering, 1980, 1981; Sessions et al., 1999; Zhang et al., 2009). The net result of these
455 factors was thought to be a virtually constant total biochemical fractionation for lipids
456 (Sternberg et al., 1984). Recent findings of different δD *n*-alkane values among plants with
457 different photosynthetic pathways that could not be explained by differences in
458 evapotranspiration have led to the recognition that combined biochemical fractionations can
459 no longer be assumed constant among plant types (Feakins and Sessions, 2010b; Polissar
460 et al., 2010; McInerney et al., 2011).

461 In addition to the similarity in $\delta D_{n\text{-}C26}$ values at similar ages in AKIII and ATI, two lines
462 of evidence suggest that our $\delta D_{n\text{-}C26}$ data unambiguously if perhaps qualitatively reflect
463 changes in precipitation despite potentially confounding influences of vegetation type and
464 other factors. First, larger changes in $\delta D_{n\text{-}C26}$ correspond in time to dry and wet intervals
465 indicated by proxies in lake sediments of eastern Africa. Second, consideration of influences
466 of vegetation changes to $\delta D_{n\text{-}C26}$ values does not alter the direction of implied precipitation
467 trends.

468 The significant shift to higher $\delta D_{n\text{-}C26}$ values after ca 6035 (MMII, Table 3, Fig. 4) is an
469 example of the first line of evidence above as it fits the time range for the end of the East
470 African humid period from a wide range of proxies in lakes and oceanic sediments (e.g.,
471 Gasse, 2000; Nyssen et al.2004, Marshall et al., 2009, 2011; Tierney et al., 2011). Dramis et
472 al. (2003) based the timing of the increase in aridity on the end of travertine/peat layer
473 formation at Mai Maikden and other nearby gullies that, like MMII was closer to ca 4500 cal y
474 BP. The $\delta^{13}C$ values at MMII shifted to less negative values at the same time as the shift in
475 $\delta D_{n\text{-}C26}$ favoring the interpretation that decreasing precipitation contributed to a relative
476 increase in C_4 plant cover. The moderate salinity of soils during the time of the shift could

have favored C_4 plants in any autochthonous inputs but unless our data are skewed by leaching, MMII had become saline well before the change in $\delta^{13}C$ values (Fig. 2). Factors other than photosynthetic pathway such as algal input and physical soil properties apparently had a negligible effect on the variation in $\delta^{13}C$ values of bulk soil organic matter so the best supported explanation for the shift in $\delta^{13}C$ values is that the proportion of biomass in C_4 plants increased at that time (Gebru et al., 2009; Terwilliger et al., 2011).

Although not systematic in direction over time, considerable variation in $\delta D_{n\text{-}C26}$ (and δD_{C3}) values in MMII occurred during the generally wetter period before ca 6000 cal y BP (Table 2; Fig. 4). The most marked oscillation from the mean for this period consisted of a large (64‰) increase that peaked at ca 7400 cal y BP. This increase closely corresponds to inferences of a dry period including this time from a variety of lacustrine microfossil proxies in eastern Africa (e.g., Stager and Mayewski, 1997; Chalié and Gasse, 2002) and supports the conclusion about magnetic and geochemical data from Lake Tana in Ethiopia that the duration of the dry period peaking at that time was short (Marshall el al., 2011).

The largest excursion in $\delta D_{n\text{-}C26}$ values after the end of the East African Humid Period occurs as a 35‰ increase beginning after 3800 and peaking at ca 3550 cal y BP in AKIII (Table 2; Fig. 5). Furthermore, magnetic susceptibility data at Lake Tana suggest that a dry period of similar duration began at 4200 cal y BP (Marshall et al., 2011). In addition, the timing of the dry period implied by our δD results is within the longer dry interval implied by valley infill characteristics elsewhere in the territory of D'MT and the Aksumite (Machado et al., 1998). Finally, this implied dry period is compatible in time with dry periods inferred for Italy, lake regions of eastern Africa, and that have been associated with the fall of sophisticated Akkadian and Egyptian cultures (Weiss et al., 1993; Hassan, 1997; Cullen et al, 2000; Gasse, 2000; Drysdale et al., 2006).

The second line of evidence that trends in our $\delta D_{n\text{-}C26}$ values unambiguously reflect changes precipitation amount is that the effects of vegetation on these values, to the best of current knowledge; do not alter the direction of these trends. Our data thus far imply large changes in forest types as well as in relative inputs of herbaceous C_4 plants (Figs. 4–6).

The largest reported difference in δD of an *n*-alkyl compound between plant groups that could have led to faulty inferences about changes in precipitation in our study sections is a 21 ‰ D enrichment in C_4 compared to C_3 grasses (Smith and Freeman, 2006; McInerney et al., 2011). We evaluated the role of change in relative contributions of C_4 cover on inferences about climate by estimating what the $\delta D_{n\text{-}C26}$ values of each sample would be if it consisted entirely of C_3 grass sources (δD_{C3}) according to the following equations.

$$\delta D_{n\text{-}C26} \text{ measured} = \rho(\delta D_{C4}) + (1-\rho)(\delta D_{C3}) \quad \textbf{[4]}$$

$$\text{and } \delta D_{C4} = \delta D_{C3} + 21 \quad \textbf{[4a]}$$

where ρ = the proportional contribution by C_4 plant sources (as calculated from [3]). Other than being lower, estimated δD_{C3} values had similar trends to those found for measured $\delta D_{n\text{-}C26}$ values (Table 2). Statistically, $\delta D_{n\text{-}C26}$ values increased by 40‰ on average from before to after ca 6035 cal y BP whereas δD_{C3} values increased by 38‰ from before to after ca 5880 cal y BP in MMII. Whereas the change in $\delta D_{n\text{-}C26}$ values from start to peak of the implied drier interval prior to ca. 6000 cal y BP at MMII was 64 ‰, the corresponding change in δD_{C3} was a negligibly larger 67 ‰. The magnitude of the change from start to peak of the largest dry interval after ca. 6000 cal y BP in AKIII was the same (35 ‰) for both $\delta D_{n\text{-}C26}$ and δD_{C3}.

Moreover, it is possible that effects of vegetation type mask an even larger decrease in precipitation at ca. 6000 cal y BP than indicated by the aforementioned raw and modeled δD values. The literature on whether δD values of *n*-alkyl groups vary systematically between woody and herbaceous plant community types is presently less consistent and subject to environmental control than the literature comparing δD values of C_3 and C_4 grasses (Bossard et al., 2011). Given that constraint, average δD values of *n*-alkanes and fatty acids of C_4 grasses (monocots) have been found to be lower than or similar to C_3 gymnosperms and dicotyledonous angiosperm tree species (e.g. for *n*-alkanes, Chikaraishi and Naraoka, 2003; Krull et al., 2006; for fatty acids, Chikaraishi et al. 2004).

Together with higher $\delta^{13}C$ values, an absence of charcoalized wood at MMII suggests that C_4-plant vegetation cover increased relative to that of C_3 plants following the $\delta D_{n\text{-}C26}$ shift at ca 6035 cal y BP (Fig 4). The combination of lower $\delta^{13}C$ values and continuous record of

533 both angiosperm and gymnosperm forest suggest that forest comprised a significant
534 component of the C_3 vegetation prior to ca 6035. Correction of this component to δD values
535 of a comparable proportion of C_3 grasses would result in inferences of even wetter times
536 during the East African Humid period than our raw data suggest. The dry interval during the
537 East African Humid period seems to have been accompanied by a switch from Angiosperm
538 tree species dominant forests to gymnosperms species dominant forests or an equal mixture
539 of both forest types. If present indications that gymnosperm trees may have higher δD *n*-
540 alkyl compound values than angiosperm trees are universally correct, then the magnitude of
541 the dry interval was lower than suggested by the raw $\delta D_{n\text{-}C26}$ value record. Present
542 indications are that if there are systematic differences in $\delta D_{n\text{-}C26}$ between gymnosperms and
543 angiosperm trees, they are not nearly large enough to erase or oppose to implication of a
544 drier interval at ca 7400 cal y BP from the MMII record. There is no indication of significant
545 forest cover in AKIII so no further indication of vegetation influences on the dry interval
546 peaking at ca 3550 cal y BP implied by the $\delta D_{n\text{-}C26}$ record there.
547 There is consensus that drier and wetter periods followed the ca 3550 cal y BP dry
548 interval but the timing of those periods remains contentious for the Plateau (Nyssen et al.,
549 2004). As synthesized in the following section, together with our other proxies, $\delta D_{n\text{-}C26}$
550 values promise more developed conclusions about the relative importances of precipitation
551 and land clearing during the times of the Plateau's most powerful civilizations than were
552 possible from other proxies that have been employed in the region.
553
554 **5.2. Environmental change and the rise and fall of D'MT and the Aksumite**
555 The δD analyses suggest that decreases in precipitation peaking at ca 7400 and
556 3550 cal y BP as well at the end of the East African Humid Period were greater than any long
557 or short-term trends during or following the times of D'MT and the Aksumite. Our results also
558 suggest that if there has been a long term drying trend (significant increase in δD) since the
559 end of the East African Humid Period, it has been slight and possibly only during the last
560 2500 years. The predicted (from segmented regression equation) increase in δD at AKIII --

561 the site with the longest continuous post-Humid Period chronology-- from ca 4400 cal y BP to
562 the present was a small 12 (for δD_{C3})–14‰ (for $\delta D_{n\text{-}C26}$) (Tables 2, 3; Fig. 5). In ATI, δD
563 values significantly increased over time but only after ca 2440 cal y BP (Tables 2, 3; Fig. 6).
564 Changes in predicted δD values from 2440 cal y BP to the present are slight and similar in
565 AKIII and ATI despite different vegetation histories. Specifically, the predicted increase over
566 this time interval was 6.5 (for δD_{C3})–8.0 ‰ ($\delta D_{n\text{-}C26}$) in AKIII and 7.4 ($\delta D_{n\text{-}C26}$)–10.8‰ (δD_{C3})
567 in ATI. Differences in predicted δD values between AKIII and ATI are small at any given
568 time, ranging from 8.0–8.6‰ for $\delta D_{n\text{-}C26}$ and further reduced to range from 1.0 –3.2‰ for
569 δD_{C3}.
570 The δD records do suggest that relatively wetter and drier short-term intervals
571 occurred during the times of D'MT and the Aksumite and that the changes in precipitation
572 during these intervals was greater than over any long-term period following the East African
573 Humid Period (Figs. 2, 5 and 6). Most notably, the emergences of both civilizations occurred
574 within modestly wetter intervals of short duration. Therefore, higher rainfall cannot be
575 discounted as an influence on the rise of the civilizations. No single pattern describes the
576 changes in precipitation during the declines of both civilizations, however.
577 Land clearing dynamics can also contribute to the complexity of polities. As indicated
578 in the following subsections, our results suggest different controls on land clearing and
579 different relationships between climate and land clearing at different times and places.
580
581 *5.2.1. Land clearing, human influence at Mai Maikden*
582 Most trends in bulk carbon isotopic, elemental, and soil micromorphological factors at
583 MMII could have occurred with time and/or with changes in precipitation amount as inferred
584 from δD values (Fig. 4). Land clearing and other decreases in biomass are possible
585 influences on these trends as well but are weaker than climate and time.
586 The relative increase in C_4 vegetation with decreasing rainfall at tropical latitudes has
587 been attributed to the increased advantage of conserving water that also limits access to
588 atmospheric CO_2 (Teeri, 1988). C_4 plants maintain high concentrations of CO_2 for productive

589 photosynthetic uptake while virtually eliminating energy consumptive photorespiration (Hatch,
590 1978). The added energy costs of C_4 photosynthesis are compensated for in environments
591 where photorespiration rates would otherwise be high due to depleted CO_2 concentrations
592 (Nobel, 1999). The concurrent increases in δD and $\delta^{13}C$ values at the end of the East
593 African Humid Period at MMII are consistent with the explanation that the shift to a drier
594 climate favored C_4 over C_3 plants (Fig. 4). Similarly, the correlation between δD and $\delta^{13}C$
595 values throughout MMII (Table 4) is consistent with the favoring of C_4 over C_3 plants as
596 rainfall decreases.

597 Trends in % area of charred organic matter (%Char Fig. 4) indicate that fire was a
598 significant component of Mai Maikden's land clearing history. The following lines of evidence
599 suggest that this history is not one of severely hot fires and furthermore that changes in
600 vegetation were most strongly linked to climate prior to the hiatus in the MMII time sequence
601 (before ca 4500 cal y BP). First, hydrogen (HI) and oxygen (OI) indices from Rock-eval
602 pyrolysis are negatively correlated suggesting that chemical changes in organic matter were
603 caused by oxidative processes such as humification (Lafargue et al., 1998; Disnar et al.,
604 2003) and/or fire of low thermal intensity. HI decreases as organic matter becomes altered,
605 while the accumulation of products from oxidation causes OI to increase. During fires of high
606 thermal severity, these products may be combusted resulting in lowered OI (Rein et al.,
607 2008).

608 Second, the combined absence of macroscopic wood fragments, low percentages of
609 TOC, and shift to higher $\%C_4$ plants in the vegetation biomass (Figs. 2, 4) suggest that Mai
610 Maikden had negligible forest cover from the end of the East African Humid Period to ca
611 4500 cal y BP and that the high %Char was herbaceous in origin. Although fire may have
612 helped to maintain the deforested condition, the shift in vegetation and precipitation (at ca
613 6000 cal y BP) occurred prior to evidence from %Char for increased burning (at ca 5600 cal
614 y BP).

615 Finally, the vegetation history of MMII prior to 6000 cal y BP includes a continuous
616 presence of closed canopy, fire intolerant juniper forests (gymnosperms in Fig. 4) and a

more intermittent presence of comparatively open canopy, fire and drought tolerant species such as *Acacia abyssinica* (Gebru et al., 2009 and angiosperms in Fig. 4). The combination of the two ecosystems further suggests that fire was never of sufficient thermal severity to completely clear the juniper forests of the East African Humid Period.

The pre-hiatus period at MMII predates D'MT—the earliest of the Plateau's known kingdoms. The lack of relationship between δD (precipitation) and %Char (fire) suggests that factors other than climate, per se, influenced fire patterns. A role of humans in land clearing then cannot be discounted, however. Land clearing by fire has been an integral practice of most ancient agricultural societies and genetic and linguistic (but not radiocarbon) analyses suggest that agricultural societies predated D'MT in the Plateau by thousands of years (Bellwood, 2005; Harrower et al., 2010).

Soils after the hiatus in MMII were younger than ca 150 cal y BP. Identified charcoalized wood indicates that the surrounding area was more forested than at either the period from ca 6000–4500 cal y BP or in today's almost entirely deforested landscape (Gebru et al., 2009). Some juniper forest remained but *Acacia* woodlands were clearly more dominant than during the East African Humid Period. Although the climate had not become too dry to support juniper forest types, climate may have influenced the change in vegetation in addition to fire patterns that continue to suggest low thermal severity. The %Char values were lower than their maximums during dry or wet portions of the pre-hiatus time interval. The relatively high HI in conjunction with low OI suggests that the organic matter had experienced minimal decomposition or burning (Disnar et al., 2003)(Fig. 4).

At no time does the total phosphorus content (Total P) record suggest intensive human influences such as urbanization or manure and fuel residue-based agriculture (Simpson et al., 2002; Adderley and Simpson, 2005; Edwards et al., 2005; Adderley et al., 2006, 2008, 2010; Filippelli et al., 2010). Agricultural activity was most likely during the time of the young, pre-hiatus soils. Total P was highest in the young mineral soil at Mai Maikden but was still lower than at the other two sites. Therefore, if there were agriculture, it did not include significant human effort to manipulate soil fertility. The older soils were reworked

travertine and peat which are typically P depleted in comparison to mineral soils (Richardson, 1985). Time and change in soil type may fully explain why Total P was highest in the youngest soils of MMII.

5.2.2. Land clearing, human influence at Adigrat

Unlike the Mai Maikden sequence, there is no evidence that changes in rainfall had a dominant, long-term influence on $\%C_4$ plant biomass or any other factor at Adigrat (Table 4). Land clearing with possible anthropogenic input may be a reason that $\%C_4$ was not correlated with climate. Not only precipitation, but also land clearing can create conditions that favor C_4 over C_3 plants (Stowe and Teeri, 1978) and anthropogenic land clearing practices can affect $\%C_4$ more than rainfall in the Ethiopian Highlands (Eshetu and Högberg, 2000; Eshetu, 2002; Terwilliger et al., 2008). During the time of D'MT, $\%C_4$ was considerably more variable than throughout the rest of the ATI chronology (Fig. 6) and this variability may best reflect rapid changes in land clearing.

Fire clearly contributed to the land clearing dynamics at Adigrat although our results suggest that fires tended to be of low thermal severity. Fire was a nearly continuous element of ATI's history as macroscopic charcoal fragments were present in all but one soil sample (Fig. 2). Furthermore, changes in tree species' composition are consistent with fire history, not rainfall. Adigrat had the most favorable climate for fire-intolerant juniper forest types but although *Juniperus procera* fragments occurred in all soils sampled for charcoal, fire-tolerant *Acacia abyssinica* was a significant component of the charcoal in all but one soil sample as well (Gebru et al., 2009; Terwilliger et al., 2011). As at Mai Maikden, the negative relationship between HI and OI at Adigrat (Table 4) could be caused by chemical changes during humification and/or fire of low thermal intensity. Time alone could have caused HI to decrease with age (Fig. 6). The increased rate of change of OI during the time of D'MT may have been caused by fires of low thermal severity, although the direction of change in OI with time then could be a consequence of decomposition alone.

Although anthropogenic activities likely explain why changes in vegetation seem to be

673 more related to land clearing than to climate; human impacts were probably light. In addition
674 to the signs that fires were of low thermal severity, %Char and %TOC were consistently too
675 low and invariant at Adigrat to suggest that humans had manipulated them to amend soil.
676 Total P was higher and may indicate a higher human influence at ATI than at Mai Maikden.
677 Total P varied little with time, however, suggesting that human impacts on soil fertility did not
678 intensify during the times of the D'MT and Aksumite peoples.
679
680 *5.2.3. Land clearing, human influence at Adi Kolen*
681 No long-term relationships were found between precipitation ($\delta D_{n\text{-}C26}$) and other
682 proxies at Adi Kolen (Table 4, Fig. 5). Instead, land-clearing pressures probably most
683 influenced some shorter-term changes in proxy values, particularly around the time of D'MT.
684 Charcoalized wood was found throughout the Adi Kolan sections suggesting a long
685 history of fire (Gebru et al., 2009; Terwilliger et al., 2011). The few charcoal fragments that
686 could be identified indicated that some fire-intolerant juniper forest existed recently.
687 Somewhat more arid climate may have contributed to the higher $\%C_4$, less forested
688 surroundings at Adi Kolen than at Adigrat (Figs. 3, 5, 6). Otherwise, most of the change in
689 $\%C_4$ during AKIII's post-hiatus history (ca 4500 cal y BP to the present) is more consistent
690 with land clearing, at times including intensified human activity, rather than a climatic
691 explanation.
692 The shift to higher $\%C_4$ after ca 3435 cal y BP occurred during the drier interval but
693 more than a century after the peak δD value at ca 3550 cal y BP (Fig. 5). This was not a lag
694 in response because $\%C_4$ increased continuously even as precipitation increased until the
695 beginning of the rise of D'MT. The simultaneous shift in other factors further suggests that
696 the increase in $\%C_4$ has other causes than climate. First, the higher %TOC in conjunction
697 with increasing $\delta D_{n\text{-}C26}$ values suggests a wetter environment that could produce more
698 biomass to burn. Second, the sharp increase in %Char indicates that fire-contributed matter
699 increased in the %TOC, while also creating conditions favoring C_4 plants by clearing land.
700 The sudden drop in OI at ca 3435 cal y BP is coupled with negligible HI values suggesting

that the organic matter was severely altered chemically but not by decomposition. Fire of higher thermal severity could produce the combination of both low HI and OI (Fig. 5).

The increase of organic matter altered by means other than humification and rich in charred sources persisted until close to the end of D'MT's time. Human manipulation alone is consistent with these results whereas there are no clear other mechanisms for producing this unusual suite of conditions. Total P was generally highest and most variable at Adi Kolan. Since this includes high values prior to ca 13500 cal y BP, it is doubtful that human influences are responsible for the abundance of Total P at Adi Kolan relative to the other sites. Nonetheless, Total P shifted to lower values at ca 3435 cal y BP, increased markedly close to the rise of D'MT, and fell in tandem with %Char and %TOC close to D'MT's decline. Total P may rise or fall as a function of fire frequency and thermal intensity (Galang et al., 2010; Resende et al., 2011). A combination of changes in fire regime and human responses to problems associated with the early drop in phosphorus may have contributed to the changes in Total P during this time.

Whether or not humans were involved, our results suggest that developments related to land clearing differed between the times of D'MT and the Aksumite at Adi Kolan: $\%C_4$ changed little during the time of Aksum, and %TOC was low as was the contribution of charred matter to it. The combined decrease in HI with time and stable, relatively high OI could be explained by humification and/or a regime of low thermal severity fire. There is no evidence, however, that the landscape was becoming heavily forested.

6. CONCLUSIONS

Combined analyses of δD values from land-plant derived fatty acid compounds (*n*-C_{26}, C_{28}, C_{30}) and other soil proxies in northern Ethiopia provided discrete insights about climate and land clearing relevant to the times of two ancient civilizations --D'MT and the Aksumite Empire. Three results suggested that the δD values yielded unambiguous records of changes in precipitation that are critical for discerning land clearing characteristics from other proxies. One showed our $\delta D_{n\text{-}C26}$ values to increase at times of droughts obtained from

729 studies of eastern African lakes. Another showed $\delta D_{n\text{-}C26}$ values in different sites to co-vary
730 during the same time intervals. Finally, correcting for one of the largest effects of plant type
731 on δD values of *n*-alkyl group molecules did not change trends in $\delta D_{n\text{-}C26}$ values with time.
732 Rainfall ($\delta D_{n\text{-}C26}$) was highest and changed the most prior to ca 6000 cal y BP. Within
733 that context, both D'MT (ca 2750–2350 cal y BP) and the Aksumite (ca 2100–1250 cal y BP)
734 arose during wetter intervals of their relatively stable and arid times. In the two sites (AKIII
735 and ATI) with time sequences spanning both civilizations, $\delta^{13}C$ values of bulk organic matter
736 were unrelated to precipitation suggesting that land clearing was a more important influence
737 than climate on relative biomasses of C_4 and C_3 plants. Charcoalized wood fragments
738 spanning long time periods in both sites suggest fire was an important agent of land clearing.
739 The $\%C_4$ plant biomass varied more during the time of D'MT than during the Aksumite
740 in both sites. Otherwise, our results suggest that characteristics of land clearing differed
741 between the two sites. Hydrogen (HI) and oxygen (OI) indices were negatively related in ATI
742 indicating that chemical alterations of organic matter were due to humification and/or fire of
743 low thermal severity. Total phosphorus contents (Total P) varied little with time and so were
744 not affected by intensified human activity specific to the support of the civilizations.
745 Our results for AKIII suggest that relatively high human impacts and fires of high
746 thermal severity affected the time of D'MT but not the Aksumite. In contrast to ATI, HI was
747 positively related to OI at AKIII. In particular, from ca 3435 to the time of D'MT's decline,
748 negligible HI indicative of severely altered organic matter was coupled to the lowest OI
749 values of our entire data set, negating the buildup of oxidized products associated with
750 humification as a cause of that alteration. Moreover, $\%C_4$ plant biomass increased with
751 decreasing precipitation and %total organic carbon as well as the contribution of charred
752 matter to it were high relative to the rest of AKIII's time sequence. An increased role of fire
753 sustained by human manipulation would produce these results. An increase in Total P
754 spanning the time of D'MT may further signal human manipulation of the landscape. The
755 time of the Aksumite suggested less severe changes in land clearance with higher OI relative
756 to HI and much lower %TOC, %Charred matter, and Total P.

757 The history of a succession of highly complex human polities makes the study region
758 a valuable natural system for testing hypotheses about repeatability of relationships between
759 environmental change and the status of civilizations. Although data are now needed closer
760 to ancient urban population centers and at higher time resolution, our results suggest that
761 some environmental changes may be more repeatable than others. The rise of both D'MT
762 and the Aksumite occurred during relatively wet intervals of the driest, least climatically
763 variable portion of the Holocene. Land clearance history apparently varied between the two
764 civilizations and between locations within their boundaries.
765

Acknowledgements

We dedicate this paper to the memory of Mohammed Umer who provided guidance in the selection of field sites and contributed intellectually to many aspects of the research. Terwilliger thanks Li Gao, then at Huang's lab, for teaching her and Tsige Gebru Kassa methods for extracting fatty acids from the soil samples and to Tsige Gebru Kassa for assistance with those extractions. Terwilliger also thanks Ying Wang and Roxane Bowden for teaching her particulars about IRMS use at Carnegie. We thank Bill Jamieson for drafting the maps of site locations for Fig. 1. The acknowledgements in Gebru et al. (2009) and Terwilliger et al. (2011) apply to this study as well. The work was funded by National Science Foundation (USA) collaborative grants to Terwilliger (BCS-0551668) and Huang (BCS-0551587).

REFERENCES

Adderley W. P. and Simpson I. A. (2005) Early-Norse home-field productivity in the Faroe Islands. *Human Ecology* **33,** 711-736.

Adderley, W. P. and Simpson, I. A. (2006) Soils and Palaeo-climate based evidence for irrigation requirements in Norse Greenland. *Journal of Archaeological Science* **33,** 1666-1679.

Adderley W. P., Simpson I. A. and Davidson D. A. (2002) Colour description and quantification in mosaic images of soil thin sections. *Geoderma* **108,** 181-195.

Adderley W. P., Simpson I. A. and Davidson D. A. (2006) Historic landscape management: a validation of quantitative soil thin-section analyses. *Journal of Archaeological Science* **33,** 320-334.

Adderley W. P., Simpson I. A. and Vésteinsson O. (2008) Local-scale adaptations: a modeled assessment of soil, landscape, microclimatic, and management factors in Norse home-field productivities. *Geoarchaeology: An International Journal* **23,** 500-527.

Adderley W. P., Wilson C. A., Simpson I. A. and Davidson, D. A. (2010) Anthropogenic Features. In *Interpretation of Micromorphological Features of Soils and Regoliths* (eds. G. Stoops, V. Marcelino and F. Mees). Elsevier, Amsterdam, pp. 569-588.

Aimers J. (2011) Drought and the Maya: The story of the artefacts. *Nature* **479,** 44.

Association of Official Agricultural Chemists. (2000) *Official methods of AOAC International,* AOAC International, Gaithersburg, MD.

Bard, KA, Coltorti M., DiBlasi M. C., Dramis F. and Fattovich R. (2000) The environmental history of Tigray (Northern Ethiopia) in the Middle and Late Holocene: a preliminary outline. *African Archaeological Review* **17,** 65-86.Beck J., Sieber A. (2010) Is the spatial distribution of mankind's most basic economic traits determined by climate and soil alone? *PLoS ONE* **5,** e10416. doi:10.1371/journal.pone.0010416.

Bellwood P. (2005) *First farmers: the origins of agricultural societies.* Blackwell, Oxford.

807 Berakhi O., Brancaccio L., Calderoni.G., Coltorti M., Dramis F. and Umer M. (1998) The Mai
808 Maiken sedimentary sequence: a reference point for the environmental evolution of
809 the highlands of northern Ethiopia. *Geomorphology* **23,** 127-138.
810 Bossard, N., J. Jacob, C. Le Milbeau, E. Lallier-Vergès, V. J. Terwilliger, R. Boscardin. 2011.
811 Variation in δD values of a single, species-specific molecular biomarker: a study of
812 miliacin throughout a field of broomcorn millet (*Panicum miliaceum* L.). *Rapid*
813 *Communications in Mass Spectrometry* 25:2732-2740.
814 Büntgen U., Tegel W., Nicolussi K., McCormick M., Frank D., Trouet V., Kaplan J. O., Herzig
815 F., Heussner K. U., Wanner H., Luterbacher J. and Esper J. (2011) 2500 years of
816 European climate variability and human susceptibility. *Science* **331,** 578-582.
817 Butzer K. W. (1981) Rise and fall of Axum, Ethiopia: a geo-archaeological interpretation.
818 *American Antiquity* **46,** 471-495.
819 Butzer K. W. (2005) Environmental history in the Mediterranean world: cross-disciplinary
820 investigation of cause-and-effect for degradation and soil erosion. *Journal of*
821 *Archaeological Science* **32,** 1773-1800.
822 CCSP. (2003) Vision for the Program and Highlights of the Scientific Strategic Plan: A
823 Report by the Climate Change Science Program and the Subcommittee on Global
824 Change Research, http://www.climatescience.gov/Library/stratplan2003/vision/ccsp-
825 vision.pdf.
826 Chalié F. and Gasse G. (2002) Late Glacial-Holocene diatom record of water chemistry and
827 lake level change from the tropical East African Rift Lake Abiyata (Ethiopia).
828 *Palaeogeography Palaeoclimatology and Palaeoecology* **187**, 259-283.
829 Chikaraishi Y. and Naraoka H. (2003) Compound specific δD—δ^{13}C analyses of *n*-alkanes
830 extracted from terrestrial and aquatic plants. *Phytochemistry* **63,** 361-371.
831 Chikaraishi Y. and Naraoka H. (2007) δ^{13}C and δD relationships among three *n*-alkyl
832 compound classes (*n*-alkanoic acid, *n*-alkane and *n*-alkanol) of terrestrial higher
833 plants. *Organic Geochemistry* **38**, 198-215.Chikaraishi Y., Naraoka H. and Poulson S.

834 R. (2004) Hydrogen and carbon isotopic fractionations of lipid biosynthesis among
835 terrestrial (C_3, C_4 and CAM) and aquatic plants. *Phytochemistry* **65**, 1369-1381.
836 Connah G. (2004) *Forgotten Africa: an Introduction to its Archaeology.* Routledge, London.
837 Cullen H. M., deMenocal P., Hemming S., Hemming G., Brown F. H., Guilderson T. and
838 Sirocko R. (2000) Climate change and the collapse of the Akkadian empire: evidence
839 from the deep sea. *Geology* **28**, 379-382.
840 Curtis M. C. (2009) Relating the Ancient Ona culture to the wider northern Horn: discerning
841 patterns and problems in the archaeology of the First Millennium BC. *African*
842 *Archaeological Review* **26,** 327-350.
843 D'Andrea A. C., Manzo A., Harrower J. J. and Hawkins A. L. (2008) The Pre-Aksumite and
844 Aksumite settlement of NE Tigrai, Ethiopia. *Journal of Field Archaeology* **33,** 151-
845 176.
846 D'Andrea A. C., Richards M. P., Pavlish L. A., Wood S., Manzo A. and Wolde-Kiros H. S.
847 (2011) Stable isotopic analysis of human and animal diets from two pre-
848 Aksumite/Proto-Aksumite archaeological sites in northern Ethiopia. *Journal of*
849 *Archaeological Science* **38,** 367-374.
850 Dansgaard W. (1964) Stable isotopes in precipitation. *Tellus* **5**, 461-469.
851 Dergachev V. A., Raspopov O. M., Damblon F., Jungner H. and Zaitseva G. I. (2007) Natural
852 climate variability during The Holocene. *Radiocarbon* **49,** 837-854.
853 deMenocal P. B. (2001) Cultural responses to climate change during the Late Holocene.
854 *Science* **292,** 667-673.
855 Diamond J. (2005) *Collapse: How Societies Choose To Fail Or Succeed.* Viking, New York.
856 DiBlasi M. C. (2005) Foreword. In *Changing Settlement Patterns in the Aksum-Yeha Region*
857 *of Ethiopia: 700 BC – AD 850* (J. W. Michels) Cambridge Monographs in African
858 Archaeology 64. BAR International Series 1446. Archaeopress Oxford, UK, pp. ix –
859 xv.Disnar J. R., Guillet B., Keravis D., Di-Giovanni C. and Sebag D. (2003) Soil
860 organic matter (SOM) characterization by Rock-Eval pyrolysis: scope and limitation.
861 *Organic Geochemistry* **34,** 327-343.

862 Disnar J. R., Jacob J., Morched-Issa M., Lottier N. and Arnaud F. (2008) Assessment of peat
863 quality by molecular and bulk geochemical analysis: application to the Holocene
864 record of the Chautagne marsh (Haute Savoie, France). *Chemical Geology* **254,** 101-
865 112.
866 Dramis F., Umer M., Calderoni G. and Haile M. (2003) Holocene climate phases from buried
867 soils in Tigray (Northern Ethiopia): Comparision with lake level fluctuations in the
868 Main Ethiopia Rifts. *Quaternary Research* **60,** 274-283.
869 Draper N. R. and Smith H. (1981) *Applied Regression Analysis (second edition).* Wiley and
870 Sons, New York.Drysdale R., Zanchetta G., Hellstrom J., Maas R., Fallick A., Pickett
871 M., Cartwright I., and Piccini L. (2006) Late Holocene drought responsible for the
872 collapse of Old World civilizations is recorded in an Italian cave flowstone. *Geology*
873 **34**, 101-104.
874 Duiker W. J. and Spielvogel J. J. (2010) *World History (sixth edition).* Wadsworth,
875 Boston.Edwards K. J., Borthwick D., Cook G., Dugmore A. J., Mairs K.-A., Church M.,
876 Simpson I. A. and Adderley W. P. (2005) A hypothesis-based approach to landscape
877 change in Suðuroy, Faroe Islands. *Human Ecology* **33,** 621-649.
878 Eglinton G. and Hamilton R. J. (1967) Leaf epicuticular waxes. *Science* **156,** 1322-1335.
879 Ehret C. (2002) *The Civilizations of Africa.* University Press of Virginia, Charlottsville.
880 Emery K. F. and Thornton E. K. (2008) A regional perspective on biotic change during the
881 Classic Maya occupation using zooarchaeological isotopic chemistry. *Quaternary*
882 *International* **191,** 131-143.
883 Enquist B. J. and Enquist C. A. F. (2011) Long-term change within a Neotropical forest
884 assessing differential functional and floristic responses to disturbance and drought.
885 *Global Change Biology* **17,** 1408-1424.
886 Eshetu Z. (2002) Historical C3-C4 vegetation pattern on forested mountain slopes: its
887 implication for ecological rehabilitation of degraded highlands of Ethiopia by
888 afforestation. *Journal of Tropical Ecology* **18,** 743-758.

889 Eshetu Z. and Högberg P. (2000) Reconstruction of forest site history in Ethiopian
890 highlands based on ^{13}C natural abundance of soils. *Ambio* **29,** 83-89.
891 Espitalié J., Deroo G. and Marquis F., (1985a) La pyrolyse Rock-Eval et ses applications :
892 première partie. *Revue de l'Institut Français du Pétrole* **40,** 563-579.
893 Espitalié J., Deroo G. and Marquis F. (1985b) La pyrolyse Rock-Eval et ses applications :
894 deuxième partie. *Revue de l'Institut Français du Pétrole* **40,** 755-784.
895 Estep M. F. and Hoering T. C. (1980) Biogeochemistry of the stable hydrogen isotopes.
896 *Geochimica et Cosmochimica Acta* **44,** 1197-1206.
897 Estep M. F. and Hoering T. C. (1981) Stable hydrogen isotope fractionations during
898 autotrophic and mixotrophic growth of microalgae. *Plant Physiology* **67**, 474-477.
899 Fattovich R. (1990) Remarks on the Pre-Aksumite Period in Northern Ethiopia. *Journal of*
900 *Ethiopian Studies* **23,** 1-34.
901 Fattovich R. (2000) The cultural and historical context. In *The Aksum Archaeological Area: a*
902 *Preliminary Assessment* (eds. R. Fattovich, K. A. Bard, L. Petrassi and V. Pisano).
903 Working Paper 1, Istituto Universitario Orientale, Napoli, pp. 21-28.
904 Fattovich R. (2009) Reconsidering Yeha, c. 800 – 400 BC. *African Archaeological Review* **26,**
905 275 – 290.
906 Feakins S. J. and Sessions A. L. (2010a) Controls on the D/H ratios of plant leaf waxes in an
907 arid ecosystem. *Geochimica et Cosmochimica Acta* **74**, 2128-2141.
908 Feakins S. J. and Sessions A. L. (2010b) Crassulacean acid metabolism influences D/H
909 ratio of leaf wax in succulent plants. *Organic Geochemistry* **41**, 1269-1276.
910 Filipelli G. M., Souch C., Horn S. P. and Newkirk D. (2010) The pre-Columbian footprint on
911 terrestrial nutrient cycling in Costa Rica: insights from phosphorus in a lake sediment
912 record. *Journal of Paleolimnology* **43,** 843-856.
913 French C., Sulas F., Madella M. (2009) New geoarchaeological investigations of the valley
914 systems in the Aksum area of northern Ethiopia. *Catena* **78,** 218-233.

915 Friis I. (1992) *Forests and forest trees of north east Tropical Africa: their natural habitats and*
916 *Distribution patterns in Ethiopia, Djibouti and Somalia.* London:Royal Botanic
917 Gardens, Kew Bulletin Additional series xv, HMSO.
918 Galang M. A., Markewitz D. and Morris L. A. (2010) Soil phosphorus transformations under
919 forest burning and laboratory heat treatments. *Geoderma* **155,** 401-408.
920 Gani N. D., Gani M. R. and Abdelsalam M. G. (2007) Blue Nile incision on the Ethiopian
921 Plateau: pulsed plateau growth, Pliocene uplift, and hominin evolution. *GSA Today*
922 **17,** 4-11.
923 Garcin Y, Schwab V. F., Gleixner G., Kahmen A., Todou G., Séné O., Onana J.-M.,
924 Achoundong G. and Sachse D.(2012) Hydrogen isotope ratios of lacustrine
925 sedimentary *n*-alkanes as proxies of tropical African hydrology: Insights from a
926 calibration transect across Cameroon. *Geochimica et Cosmochimica Acta* **79,** 106-
927 126.
928 Gasse F. (2000) Hydrological changes in the African tropics since the Last Glacial Maximum.
929 *Quaternary Science Reviews* **19**, 189-211.
930 Gat J. R. (1980) The isotopes of hydrogen and oxygen in precipitation. In *Handbook of*
931 *Environmental Isotope Geochemistry* **1,** 21-47.
932 Gebru T., Eshetu Z., Huang Y., Woldemariam T., Strong N., Umer M,. DiBlasi M. and
933 Terwilliger V. J. (2009) Holocene palaeovegetation of the Tigray Plateau in northern
934 Ethiopia from charcoal and stable organic carbon isotopic analyses of gully
935 sediments. *Palaeogeography, Palaeoclimatology, and Palaeoecology* **282,** 67-80.
936 Gelfand M. J., Raver J. L., Nishii L., Leslie L. M., Lun J., Lim B. C., Duan L., Almaliach A.,
937 Ang S., Arnadottir J., Aycan Z., Boehnke K., Boski P., Cabecinhas R., Chan D.,
938 Chhokar J., D'Amato A., Ferrer M., Fischlmayr I. C., Fischer R., Fülöp M., Georgas J.,
939 Kashima E. S., Kashima Y., Kim K., Lempereur A., Marquez P., Othman R., Overlaet
940 B., Panagiotopoulou P., Peltzer K., Perez-Florizno L. R., Ponomarenko L., Realo A.,
941 Schei V., Schmitt M., Smith P. B., Soomro N., Szabo E., Taveesin N., Toyama M.,

942 Van de Vliert E., Vohra N., Ward C. and Yamaguchi S. (2011) Differences Between
943 Tight and Loose Cultures: A 33-Nation Study. *Science* **332,** 1100–1104.
944 Giorgi F., Diffenbaugh N. S., Gao X. J., Coppola E., Dash S. K., Frumento O., Rauscher S.
945 A., Remedio A., Sanda I. S., Steiner A., Sylla B. and Zekey A. S. (2008) The regional
946 climate change hyper-matrix framework. *EOS* **89,** 445-446.
947 Harrower MJ, McCorriston J and D'Andrea AC. (2010) General/specific, local/global:
948 comparing the beginnings of agriculture in the Horn of Africa (Ethiopia/Eritrea) and
949 Southwest Arabia (Yemen). *American Antiquity* **75,** 452-472.
950 Hassan R. (1997) Nile floods and political disorder in early Egypt. In *Third millennium B.C.*
951 *Climate Change and Old World Collapse* (ed. H. N. Dalfes). Springer, Berlin, **49,** pp.
952 1-23.
953 Hatch M. D. (1978) Regulation of enzymes in C_4 photosynthesis. *Current Topics in Cellular*
954 *Regulation* **14,** 1-27.
955 Haug G. H., Günther D., Peterson L. C., Sigman D. M., Hughen K. A. and Aeschlimann B.
956 (2003) Climate and the collapse of Maya civilization. *Science* **299,** 1731-1735.
957 Hodell D. (2011) Drought and the Maya: Maya megadrought? *Nature* **479,** 44.
958 Hou J., D'Andrea W. J. and Y. Huang. (2008) Can sedimentary leaf waxes record D/H
959 ratios of continental precipitation? Field, model, and experimental assessments.
960 *Geochimica et Cosmochimica Acta* **72,** 3503-3517.
961 IPCC-Intergovernmental Panel on Climate Change. (2007) Climate change 2007: the
962 physical science basis. Contribution of Working Group I to the Fourth Assessment
963 Report of the IPCC, Geneva. (eds. S. Solomon, D. Qin, M. Manning, Z. Chen, M.
964 Marquis, K. B. Avery, M. Tignor and H. L. Miller, eds.) Cambridge University Press,
965 Cambridge, UK. http://www.ipcc.ch/publications_and_data/ar4/wg1/en/contents.html .
966 Jackson P. C., Meinzer F. C., Bustamante M., Goldstein G., Franco A., Rundel P. W., Caldas
967 L., Igler E. and Causin F. (1999) Partitioning of soil water among tree species in a
968 Brazilian Cerrado ecosystem. *Tree Physiology* **19,** 717-724.

969 Jones D., Briffa K. R., Osborn T. J., Lough J. M., van Ommen T. D., Vinther B. M.,
970 Luterbacher J., Wahl E. R., Zwiers F. W., Mann M. E., Schmidt G. A., Ammann C. M.,
971 Buckley B. M., Cobb K. M., Esper J., Goosse H., Graham N., Jansen E., Kiefer T.,
972 Kull C., Küttel M., Mosley-Thompson E., Overpeck J. T., Riedwyl N., Schulz M.,
973 Tudhope A. W., Villalba R., Wanner H., Wolff E. and Xoplaki E. (2009) High-
974 resolution palaeoclimatology of the last millennium: a review of current status and
975 future prospects. *The Holocene* **19,** 3-49.
976 Kolattukudy P. E. (1970) Biosynthesis of cuticular lipids. *Annual Review of Plant Physiology*
977 **21,** 163-192.
978 Krull E., Sachse D., Mügler I, Thiele A., Gleixner G. (2006) Compound-specific $\delta^{13}C$ and $\delta^{2}H$
979 analyses of plant and soil organic matter: A preliminary assessment of the effects of
980 vegetation change on ecosystem hydrology. *Soil Biology & Biochemistry* **38,** 3211–
981 3221.
982 Lafargue E., Marquis F. and Pillot D. (1998) Rock-Eval 6 applications in hydrocarbon
983 exploration, production, and soil contamination studies. *Revue de l'Institut Français*
984 *du Pétrole* **53,** 421-437.
985 Machado M. J., Perez-Gonzalez, A. and Benito G. (1998) Paleoenvironmental changes
986 during the last 4000 years in the Tigray, northern Ethiopia. *Quaternary Research* **49**,
987 312-321.
988 Marshall M. H., Lamb H. F., Davies S. J., Leng M. J., Kubsa Z., Umer M. and Bryant, C.,
989 (2009) Climatic change in northern Ethiopia during the past 17,000 years: a diatom
990 and stable isotope record from Lake Ashenge. *Palaeogeography, Palaeoclimatology,*
991 *Palaeoecology* **279,** 114-17.
992 Marshall M. H., Lamb H. F., Huws D., Davies S. J., Bates R., Bloemendal J., Boyle J. Leng
993 M. J., Umer M. and Bryant C. (2011) Late Pleistocene and Holocene drought events
994 at Lake Tana, the source of the Blue Nile. *Global and Planetary Change* **78**, 147-161.
995 Mastrandrea M.D. and Schneider S.H. (2010). *Preparing for Climate Change.* MIT Press,
996 Cambridge, MA.

997 McGovern T. H. (1994) Management for Extinction in Norse Greenland. *In Historical*
998 *Ecology: Cultural Knowledge and Changing Landscapes* (ed. C. Crumley). Santa Fe
999 School of American Research Monograph, pp. 127-154.
1000 McInerney F. A., Helliker B. R. and Freeman K. H. (2011) Hydrogen isotope ratios of leaf
1001 wax *n*-alkanes in grasses are insensitive to transpiration. *Geochimica et*
1002 *Cosmochimica Acta* **75**, 541-554.
1003 Munsell Soil Color Charts. (1994) Macbeth Division of Kollmorgen Instruments Corporation,
1004 New Windsor, NY.
1005 Murphy C. P. (1984) The overestimation of clay and the underestimation of pores in soil thin-
1006 sections. *Journal of Soil Science* **35,** 481-495.
1007 National Meteorological Agency of Ethiopia. (1998-2006) Available through
1008 http://www.ethiomet.gov.et/stations/regional_information/1.
1009 Niedermeyer E. R., Schefuss E., Sessions A. L., Mulitza S., Mollenhauer G., Schulz M. and
1010 Wefer G. (2010) Orbital- and millennial-scale changes in the hydrologic cycle and
1011 vegetation in the western African Sahel: insights from individual plant wax δD and
1012 $\delta^{13}C$. *Quaternary Science Reviews* **29**, 2996–3005.
1013 Nobel, P.S. (1999) *Physicochemical and Environmental Plant Physiology, 2nd edition.*
1014 Academic Press, San Diego.
1015 Nyssen J., Poesen J., Moeyersons J., Deckers J., Haile M. and Lang A., (2004) Human
1016 impact on the environment in the Ethiopian and Eritrean highlands-a state of the art.
1017 *Earth Science Reviews* **64,** 273-320.
1018 Oosterbaan R. J. (no date) http://www.waterlog.info/segreg.htm.
1019 Oosterbaan R. J., Sharma D. P., Singh K. N. and Rao K. V. G. K. (1990) Crop production
1020 and soil salinity: evaluation of field data from India by segmented linear regression
1021 with breakpoint. Session V, Proceedings of the Symposium on Land Drainage for
1022 Salinity Control in Arid and Semi-Arid Regions, Cairo, February 1990 **3,** 373-383.

1023 Patterson W. P., Dietrich K. A., Holmden C. and Andrews J. T. (2010) Two millennia of
1024 North Atlantic seasonality and implications for Norse colonies. *Proceedings of the*
1025 *National Academy of Sciences* **107,** 5306-5310.
1026 Phillipson D. W. (1998) *Ancient Ethiopia, Aksum: its Antecedents and Successors.* British
1027 Museum Press, London.
1028 Polissar P. J., Freeman K. H. (2010) Effects of aridity and vegetation on plant-wax δD in
1029 modern lake sediments. *Geochimica et Cosmochimica Acta* **74**, 5785-5797.
1030 Reimer P. J., Baillie M. G. L., Bard E., Bayliss A., Beck J. W., Bertrand C. J. H., Blackwell P.
1031 G., Buck C. E., Burr G. S., Cutler K.B., Damon P.E., Edwards R.L., Fairbanks R.G.,
1032 Friedrich M., Guilderson T. P., Hogg A.., Hughen K. A., Kromer B., McCormac G.,
1033 Manning S., Ramsey C. B., Reimer R. W., Remmele S., Southon J. R., Stuiver M.,
1034 Talamo S., Taylor F. W., van der Plicht J., Weyhenmeyer C. E. (2004) INTCAL04
1035 terrestrial radiocarbon age calibration, 0 - 26 cal kyr BP. *Radiocarbon* **46,** 1029–1058.

1036 Rein G., Cleaver N., Ashton C., Pironi P., and Torero J. (2008) The severity of smouldering
1037 peat fires and damage to the forest soil. *Catena* **74,** 304-309.
1038 Resende J. C. F., Markewitz D., Klink C. A., Bustamante M. M. da C. and Davidson E. A.
1039 (2011) Phosphorus cycling in a small watershed in the Brazilian Cerrado: impacts of
1040 frequent burning. *Biogeochemistry* **105,** 105-118.
1041 Rhoades J. D. and Corwin D. L. (1993) Electrical conductivity methods for measuring and
1042 mapping soil salinity. *Advances in Agronomy* **49,** 201–251.
1043 Richardson C. J. (1985) Mechanisms controlling phosphorous retention capacity in
1044 freshwater wetlands. *Science* **228,** 1424-1427.
1045 Risi C., Bony S. and Vimeux F. (2008) Influence of convective processes on the isotopic
1046 composition ($\delta^{18}O$ and δD of precipitation and water vapor in the tropics: 2. Physical
1047 interpretation of the amount effect. Journal of Geophysical Research 113,
1048 doi:10.1029/2008JD009943.

1049 Robin C. and de Maigret A. (1998) Le Grand Temple de Yéha (Tigray, Ethiopie), après la
1050 première campagne de fouilles de la Mission française (1998). *Comptes-rendus des*
1051 *Séances de l'Académie des Inscriptions et Belles-Lettres* **142,** 737-798.
1052 Ruben S., Randall M., Kamen M. D. and Hyde J. L. (1941) Heavy oxygen (^{18}O as tracer in
1053 the study of photosynthesis. *Journal of the American Chemical Society* **63,** 877-878.
1054 Sachse D., Radke J., and Gleixner G. (2004) Hydrogen isotope ratios of recent lacustrine
1055 sedimentary *n*-alkanes. *Geochimica et Cosmochimica Acta* **68,** 4877-4889.
1056 Sachse D., Radke J., and Gleixner G. (2006) δD values of individual n-alkanes from
1057 terrestrial plants along a climatic gradient—Implications for the sedimentary
1058 biomarker record. *Organic Geochemistry* **37,** 469-483.
1059 Sachse D., Billault I., Bowen G. J., Chikaraishi Y., Dawson T. E., Feakins S. J., Freeman K.
1060 H., Magill C. R., McInerney F. A., van der Meer B. T. J., Polissar P., Robins R. J.,
1061 Sachs J. P., Schmidt H.-L., Sessions A. L., White J. W. C., West J. B. and Kahmen A.
1062 (2012) Molecular paleohydrology: interpreting the hydrogen-isotopic composition of
1063 lipid biomarkers from photosynthesizing organisms. *Annual Review of Earth and*
1064 *Planetary Sciences* **40,** 221-249.
1065 Schoeneberger P. J., Wysocki D. A., Benham E. C. and Broderson, W. D. (eds), 2002.
1066 *Field book for describing and sampling soils,* Version 2.0. Natural Resources
1067 Conservation Service, National Soil Survey Center, Lincoln, NE.
1068 Sessions A. L., Burgoyne T. W., Schimmelmann A., and Hayes J. M. (1999) Fractionation of
1069 hydrogen isotopes in lipid biosynthesis. *Organic Geochemistry* **30**, 1193-1200.
1070 Simpson I. A., Adderley W. P., Guðmundsson G., Hallsdóttir, Sigurgeirsson M. Á. and
1071 Snæsdóttir M. (2002) Soil limitations to agrarian land production in premodern
1072 Iceland. *Human Ecology* **30,** 423-443.
1073 Simpson I. A., Vesteinsson O., Adderley W. P. and McGovern T. H. (2003) Fuel resource
1074 utilisation in landscapes of settlement. *Journal of Archaeological Science* **30,** 1401-
1075 1420.
1076

1077 Smith F. A. and Freeman K. H. (2006) Influence of physiology and climate on δD of leaf wax
1078 *n*-alkanes from C_3 and C_4 grasses. *Geochimica et Cosmochimica Acta* **70**, 1172-
1079 1187.
1080 Soil Survey Staff., (1995) *Soil Survey Laboratory Information Manual. USDA, Natural*
1081 *Resources Conservation Service, Soil Survey Investigations Report No. 45, Version*
1082 *1.0.* National Soil Survey Center. Lincoln, NE.
1083 Sokal R. R. and Rohlf F. J. (1995) *Biometry: the Principles and Practice of Statistics in*
1084 *Biological Research (third edition).* Freeman, New York.
1085 Stager J. C. and Mayewski P. A. (1997) Abrupt early to mid-Holocene climatic transition
1086 registered at the equator and the poles. *Science* **276**, 1834–1836.
1087 Sternberg L. S. L. (1989) Oxygen and hydrogen isotope ratios in plant cellulose: mechanisms
1088 and applications. In *Stable Isotopes in Ecological Research* (eds. P. W. Rundel, J. R.
1089 Ehleringer and K. A. Nagy) Springer , New York, pp. 124–141.
1090 Sternberg L., DeNiro M. J. and Agie H. (1984) Stable hydrogen isotope ratios of saponifiable
1091 lipids and cellulose nitrate from CAM, C_3 and C_4 plants. *Phytochemistry* **23**, 2475-
1092 2477.
1093 Stowe L. G. and Teeri J. A. (1978) The geographic distribution of C_4 species of the
1094 dicotyledonae in relation to climate. *American Naturalist* **112,** 609-623.
1095 Stuiver M. and Reimer, P. (1986-2005) CALIB 5.0.2. http://calib.qub.ac.uk/calib.
1096 Stuiver M. and Reimer P. (1993) Extended ^{14}C data base and revised calib 3.0 ^{14}C age
1097 calibration program. *Radiocarbon* **35,** 215-230.
1098 Sulas F. (2010) Environmental and cultural interplay in highland Ethiopia: geoarchaeology at
1099 Aksum. Ph. D. thesis, University of Cambridge, Department of Archaeology,
1100 Cambridge, UK.
1101 Teeri J. (1988) Interaction of temperature and other environmental variables influencing
1102 plant distribution. *Symposia of the Society for Experimental Biology* **42,** 77–89.
1103 Telford J. J., Heegaard E., and Birks H. M. B. (2004) The intercept is a poor estimate of a
1104 calibrated radiocarbon age. *The Holocene* **14,** 296–298.

Terwilliger V. J., Eshetu Z., Alexandre M., Huang Y., Umer M. and Gebru T. (2011) Local variation in climate and land use during the time of the major kingdoms of the Tigray Plateau of Ethiopia and Eritrea. *Catena* **85,** 130-143.

Terwilliger V.J., Eshetu Z., Colman A., Bekele T., Gezahgne A. and Fogel M.L. 2008. Reconstructing palaeoenvironment from $\delta^{13}C$ and $\delta^{15}N$ values of soil organic matter: a calibration from arid and wetter elevation transects in Ethiopia. *Geoderma* **147,** 197-210.

Thomson D. J. (1990) Time series analysis of Holocene climate data. *Philosophical Transactions of the Royal Society of London. Series A, Mathematical and Physical Sciences* **330,** 601-616.

Tierney J., Lewis S. C., Cook B. I., LeGrande A. N. and Schmidt G. A. (2011) Model, proxy and isotopic perspectives on the East African Humid Period. *Earth and Planetary Science Letters* **307**, 103-112.

Trouve C., Mariotti A., Schwarz D. and Geuillet, B. (1994) Soil organic carbon dynamics under Eucalyptus and Pinus planted on savanna in the Congo. *Soil Biology and Biochemistry* **26,** 287-295.

Turchin P. (2008) Arise 'cliodynamics'. *Nature* **454,** 34-35.

Vimeux F., Masson V., Jouzel J., Stievenard M. and Petit J. R. (1999) Glacial-interglacial changes in ocean surface conditions in the southern hemisphere. *Nature* **398,** 410-413.

Weiss H. and Bradley S. (2001) What drives societal collapse? *Science* **291,** 609-610.

Weiss H., Courty M. A., Wetterstrom W., Guichard F., Senior L., Meadow T., and Curnow A. (1993). The genesis and collapse of third millennium North Mesopotamian civilization. *Science* **261**, 995-1004.

Whalley W. R., Riseley B., Leeds-Harrison P. B., Bird N. R. A., Leech P. K. and Adderley W. P. (2005) Structural differences between bulk and rhizosphere soil. *European Journal of Soil Science* **56,** 353-360.

1132 Worden J., Noone D. and Bowman K. (2007) Importance of rain evaporation and continental
1133 convection in the tropical water cycle. *Nature* **445,** 528-532.
1134 Yakir, D. (1992) Variations in the natural abundance of oxygen-18 and deuterium in plant
1135 carbohydrates. *Plant, Cell and Environment* **15**, 1005-1020.
1136 Yurtsever Y. (1975) Worldwide survey of stable isotopes in precipitation. *Report Section*
1137 *Isotope Hydrology*. International Atomic Energy Association, Vienna.
1138 Zhang X., Gillespie A. L. and Sessions A. (2009) Large D/H variations in bacterial lipids
1139 reflect central metabolic pathways. *Proceedings of the National Academy of*
1140 *Sciences* **106**, 12580-12586.
1141

Figure legends.

Figure 1. Locations of study sites and sequences.

Figure 2. Lithology and salinity related characteristics of study sections at Adi Kolen (AKIII), Adigrat (ATI), and Mai Maikden (MMII).Closed circles indicate where charcoalized wood was found and dates are those used to estimate age-depth relationships (see text). Open circles indicate samples where charcoal was not found. The arrows in AKIII and MMII point to unconformities with large associated hiati in time. Interpolated dates used to estimate rate changes indicated by lithology are marked with an X. Rjck fragment modifiers accompanying texture names follow the USDA classification where in a total soil sample, 15%≤gravelly or cobbly<35% and 60%≤extremely gravelly or cobbly (Soil Survey Staff, 1995). The two columns per section of soil physical properties are modified from Gebru et al., (2009) and Terwilliger et al. (2011).

Figure 3. $\delta D_{n\text{-}C26}$ values (‰ VSMOW), $\delta^{13}C$ of bulk organic matter (‰ PDB), and estimated $\%C_4$ plant of total plant-derived C in all three sections. Closed circles connected by solid lines are for the section at Adi Kolan (AKIII), open circles connected by long dashed lines are for the Mai Maikden section MMII, and x symbols connected by short dashed lines are for the Adigrat section ATI. The plots of $\delta^{13}C$ are modified from Gebru et al. (2009) and Terwilliger et al. (2011).

Figure 4. Trends in $\delta D_{n\text{-}C26}$ and bulk organic $\delta^{13}C$ values (A) with accompanying non-isotopic factors in MMII. $\%C_4$ is estimated $\%C_4$ plant of total plant-derived C ,TOC is total organic carbonand Identified charcoal % is the % of all identifiable charcoalized wood fragments in a sample that were from the indicated vegetation type (A). HI and OI are hydrogen and oxygen indices from Rock-Eval pyrolysis, Total P is phosphorus content, and Char is charred matter (B). Open circles indicate data used for correlation analyses with other factors. In

1170 factors where these values were only a subset of the all the data analyzed ($\delta^{13}C$ and %TOC),
1171 the remaining data are shown as closed black symbols. Short-dashed, dark gray lines
1172 indicate significant, long-term trends in all values of a factor over time. In the factors where
1173 data subsets were used in segmented regression analyses (not identified charcoal%); short
1174 dashed black lines indicate the long-term trends of the data subsets. The plots of $\delta^{13}C$,
1175 %TOC, and Identified charcoal % are modified from Gebru et al. (2009).
1176
1177 **Figure 5**. Trends in $\delta D_{n\text{-}C26}$ and bulk organic $\delta^{13}C$ values, and accompanying non-isotopic
1178 factors in AKIII. See Fig. 4 for explanation of lines and labels. The plots of $\delta^{13}C$, %TOC, nd
1179 Identified charcoal % are modified from Gebru et al. (2009) and Terwilliger et al. (2011).
1180
1181 **Figure 6**. Trends in $\delta D_{n\text{-}C26}$ and bulk organic $\delta^{13}C$ values with accompanying non-isotopic
1182 factors in ATI. See Fig. 3 for explanation of lines and labels. The plots of $\delta^{13}C$, %TOC, nd
1183 Identified charcoal % are modified from Gebru et al. (2009) and Terwilliger et al. (2011).

Appendix A

Dry structure, structure grade, consistence, and color data for study sections presented in this paper. The structural and consistence descriptions were developed from the guidelines in Schoeneberger et al. (2002). Color descriptions, hue, value, and chroma were determined from Munsell Soil Color Charts (1994). The data from AKIII and ATI can also be found in the Supplemental materials of Terwilliger et al., (2011).

Section	Depth (cm)	Structure	Grade	Consistence	Color	Hue Value/Chroma
AKIII	0	granular	structureless-weak	soft	yellowish brown	10YR 5/8
	30	granular	weak	soft	yellowish brown	10YR 5/6
	60	granular-subangular blocky	weak-moderate	slightly hard	yellowish brown	10YR 5/4
	100	granular-subangular blocky	weak-moderate	slightly hard	dark yellowish brown	10YR 4/3
	130	granular-subangular blocky	weak-moderate	slightly hard	dark yellowish brown	10YR 4/3
	160	granular-subangular blocky	weak-moderate	slightly hard	dark yellowish brown	10YR 4/3
	190	granular-subangular blocky	weak-moderate	soft-slightly hard	dark yellowish brown	10YR 4/3
	220	subangular blocky	moderate	moderately hard	dark yellowish brown	10YR 4/3
	270	granular-subangular blocky	weak-moderate	slightly-moderately hard	dark yellowish brown	10YR 4/3
	295	subangular blocky	moderate-strong	hard	dark brown	7.5YR 3/2
	305	subangular blocky	moderate	moderately hard	dark brown	7.5YR 3/2
	320	subangular blocky	moderate-strong	hard	dark brown	7.5YR 3/2
	360	granular-subangular blocky	moderate	moderately hard	very dark brown	7.5YR 2.5/2
	440	subangular blocky	moderate-strong	hard	dark brown	7.5YR 3/2
	470	granular-subangular blocky	moderate	hard	yellowish brown	10YR 5/4

	490	granular-subangular blocky	weak-moderate	slightly-moderately hard	brownish yellow	10YR 6/6
	510	granular-subangular blocky	weak-moderate	soft-slightly hard	light yellowish brown	10YR 6/4
	540	subangular blocky	moderate-strong	hard	dark grayish brown	10YR 4/2
	560	granular-subangular blocky	weak-moderate	slightly-moderately hard	yellowish brown	10YR 5/4
	580	granular-subangular blocky	weak	soft	brownish yellow	10YR 6/6
	620	granular	weak	loose-soft	brownish yellow	10YR 6/8
	660	granular	weak	loose-soft	brownish yellow	10YR 6/8
MM ll	0	granular	structureless	loose-soft	dark yellowish brown	10YR 4/4
	10	granular-subangular blocky	structureless-weak	loose-soft	yellowish brown	10YR 5/4
	20	subangular blocky	moderate	moderately hard	yellowish brown	10YR 5/4
	30	subangular blocky	weak	slightly hard	dark grayish brown	10YR 4/2
	35	subangular blocky	weak	slightly hard	grayish brown	10YR 5/2
	45	subangular blocky	weak	slightly hard	grayish brown	10YR 5/2
	60	sub-angular blocky	weak	slightly-moderately hard	light gray	10YR 7/2
	90	granular-subangular blocky	structureless-weak	loose-soft	light gray	10YR 7/2
	100	subangular blocky	weak	moderately hard	greenish gray	gley 4/1 10Y
	110	subangular blocky	weak	slightly hard	dark greenish gray	gley 3/1 10Y
	115	subangular blocky	weak	slightly hard	pale red	2.5YR 7/2
	130	subangular blocky	weak	slightly hard	reddish gray	2.5YR 5/1
	155	subangular blocky	weak	slightly hard	light greenish gray	gley 7/1 10Y
	170	angular blocky	weak	moderately hard	gray	gley 5/N

180	subangular blocky	weak	slightly hard	greenish gray	gley 5/1 10Y
190	subangular blocky	weak	slightly hard	greenish gray	gley 6/1 10Y
200	subangular blocky	weak	slightly hard	light greenish gray	gley 7/1 10Y
220	subangular blocky	weak	slightly hard	light gray	5Y 7/2
230	subangular blocky	weak	moderately hard	light gray	5Y 7/2
245	angular blocky	weak	slightly hard	greenish gray	gley 6/1 10Y
250	subangular blocky	weak	slightly hard	light gray	5Y 7/2
280	subangular blocky	weak	soft	greenish gray	gley 5/1 5GY
300	subangular blocky	weak	slightly hard	light gray	10R 7/1
310	subangular blocky	weak	moderately hard	pale red	10R 7/2
320	angular blocky	weak	slightly hard	dark greenish gray	gley 4/1 10Y
330	subangular blocky	weak	moderately hard	dark greenish gray	gley 3/1 10Y
340	granular	structureless-weak	loose-soft	strong brown	7.5YR 5/8
355	angular blocky	weak	slightly hard	very dark gray	gley 3/N
360	granular	structureless-weak	loose-soft	light gray	10YR 7/1
370	subangular blocky	weak	moderately hard	dark greenish gray	gley 3/1 10Y
380	angular blocky	weak	slightly hard	very dark gray	gley 3/N
386	granular	structureless-weak	loose-soft	light gray	10YR 7/1
390	subangular blocky	weak	soft	gray	10YR 6/1
400	angular blocky	weak	slightly hard	very dark gray	gley 3/N
414	subangular blocky	weak	soft	gray	10YR 6/1
425	granular	structureless-weak	loose-soft	light gray	5YR 7/1
470	subangular blocky	weak	moderately hard	pinkish gray	5YR 7/2
480	granular	structureless-weak	loose-soft	light gray	10YR 7/1

	510	subangular blocky	weak	slightly hard	pinkish gray	5YR 7/2
	530	subangular blocky	weak	slightly hard	light gray	5YR 7/1
	540	subangular blocky	weak	moderately hard	pinkish gray	5YR 7/2
	550	angular blocky	weak	slightly hard	very dark gray	gley 3/N
	560	granular	structureless	loose	pinkish gray	7.5YR 7/2
	580	subangular blocky	weak	slightly hard	light gray	5YR 7/1
	595	angular blocky	weak	hard	gray	5YR 5/1
	640	angular blocky	weak	slightly hard	very dark gray	gley 3/N
ATI	0	granular-subangular blocky	weak-moderate	loose-soft	yellowish brown	10YR 5/6
	100	granular-subangular blocky	moderate	slightly hard	dark yellowish brown	10YR 4/4
	130	granular-subangular blocky	weak-moderate	slightly hard	dark yellowish brown	10YR 4/4
	180	granular-subangular blocky	weak-moderate	slightly-moderately hard	dark yellowish brown	10YR 4/6
	210	subangular blocky	moderate	moderately hard	yellowish brown	10yr 5/4
	250	granular-subangular blocky	weak-moderate	slightly hard	yellowish brown	10YR 5/6
	310	single grain-granular	structureless-weak	slightly-moderately hard	light yellowish brown	10YR 6/4
	320	granular-subangular blocky	weak	slightly hard	light yellowish brown	10YR 6/4
	360	single grain-granular	structureless-weak	loose	pale brown	10YR 6/3
	370	granular-subangular blocky	weak	soft	light yellowish brown	10YR 6/4
	430	granular-subangular blocky	structureless-weak	soft	light yellowish brown	10YR 6/4
	470	single grain	structureless	loose	brownish yellow	10YR 6/6

Table 1. Radiocarbon and calibrated calendar dates of sections at Adi Kolen, Mai Maikden, and Adigrat.

Site	Section	Depth (cm)	UCIAMS #	Radiocarbon age (^{14}C yr BP)	Calibrated age range (cal yr BP) (2 σ, 95.4%)	Relative area under distribution	Median age from probability distribution (cal yr BP)
Adi Kolan	AKIII	30	53894	105±15	27–47, 55–140, 221–259	0.119, 0.595, 0.285	113
		100	36088	855±15	788–731	1.000	759
		220	36089	2345±15	2356–2340	1.000	2349
		305	36090	2420±20	2491–2354, 2607–2603, 2677–2642	0.899, 0.005, 0.096	2429
		360	53897	3890±15[a]	4250–4274, 4284–4413	0.075, 0.925	4343
		540	36091	3600±15	3931–3847, 3970–3942	0.817, 0.183	3903
		620	53895	12035±30	13793–1399030	1.000	13887
		660	36109	11735±25	13701–13597	1.000	13597
Mai Maikden	MMII	30	36111	130±15	-1–-3, 41–12, 148–60, 199–187, 233–211, 269–241	0.002, 0.168, 0.519, 0.024, 0.118, 0.169	112
		320	36124	5640±100[b]	6228–6223, 6664–6277	0.002, 0.998	6437
		385	36100	6130±15	7029–6946, 7069–7051, 7084–7078, 7156–7098	0.663, 0.029, 0.006, 0.302	7005
		470	36101	6625±20	7568-7469	1.000	7519
		575	36102	7055±20	7941-7844	1.000	7892
Adigrat	ATI	000	53896	395±15	336–348, 454–505	0.06, 0.94	485
		100	36092	1345±15	1298–1269	1.000	1287
		210	36110	1045±15[a]	969-929	1.000	949
		360	36093	2460±15	2414–2364, 2545–2433, 2572–2561, 2617–2584, 2701–2635	0.084, 0.375, 0.017, 0.144, 0.381	2591
		470	36094	2680±15	2794–2752, 2843–2823	0.926, 0.074	2773

All analyses were performed at the University of California Irvine Keck Carbon Cycle Accelerator Mass Spectrometry lab, Earth System Science Department (UCIAMS). Size-dependent sample preparation backgrounds were subtracted based on measurements of ^{14}C-free wood. Radiocarbon ages were corrected for isotopic fractionation according to the conventions of Stuiver and Polach (1977), with $\delta^{13}C$ values measured on prepared graphite using the AMS. These can differ from $\delta^{13}C$ of the original material, if fractionation occurred during sample graphitization or the AMS measurement, and are not shown. All of the dated samples were charcoalized wood. Radiocarbon ages were calibrated using CALIB v5.0.2 (Stuiver and Reimer, 1993) using the INTCAL04.14c dataset (Reimer et al. 2004). All samples were charcoal. This table shows data from Table 2 of Gebru et al. (2009) and Table 1 of Terwilliger et al (2011).

[a] Samples suggest redeposition.

[b]The large uncertainty is due to the very small sample size (0.025 mg).

Table 2. δD values of land-plant derived fatty acids, date matched bulk organic $\delta^{13}C$values, and elemental and charred organic matter contents.

Depth	Age	δD (‰)				$\delta^{13}C$ bulk	%TOC	HI (mg HC	OI (mg O_2	Total P	%Char
(cm)	(cal y BP)	*n*-C_{26}	*n*-C_{28}	*n*-C_{30}	C_3 corr	(‰)	(gC g^{-1})	g^{-1} TOC)	g^{-1} TOC)	(mg kg^{-1})	(% area)
1. Mai Maikden (MMII)											
0	100	-127	-132	-114	-139	-20	2.3	140	369	857	7.3
30	112	-157	-131	-133	-172	-18	1.4	100	381	890	28.0
100	4515	-152	-147	-148	-166	-18	1.3	20	358	475	13.3
115	4646	n.a.	n.a.	n.a.	n.a.	-19	0.6	0	1049	150	0.3
130	4777	-163	-140	-139	-176	-19	0.6	0	1025	184	53.2
145	4908	n.a.	n.a.	n.a.	n.a.	n.a.	n.a.	0	1236	147	34.5
170	5126	-133	-162	-156	-144	-20	1.3	49	396	628	10.4
200	5388	-153	-160	-176	-165	-19	0.7	16	893	283	68.5
220	5563	-160	-170	-161	-173	-19	0.9	21	693	253	44.9
250	5825	-136	-143	n.a.	-154	-16	0.6	10	1423	238	0.1
270	6000	-166	-141	-158	-186	-13	1.4	21	378	144	0.0
300	6262	-203	-184	-158	-212	-23	1.3	82	320	112	5.2
320	6437	-204	-197	-174	-213	-22	4.3	81	296	297	21.8
355	6743	-209	-200	-196	-219	-22	5.5	101	321	419	46.3
380	6961	-211	-198	-168	-226	-17	6.0	79	276	376	50.1
400	7096	-198	-194	-189	-207	-22	6.4	48	236	640	55.8
425	7247	-185	-158	-132	-194	-22	0.6	44	432	184	0.3
450	7398	-126	n.a.	-131	-135	-22	0.4	49	479	169	0.0
470	7519	-173	-170	-161	-183	-22	0.7	44	418	182	1.6
500	7626	-190	-194	-183	-203	-19	1.0	30	341	243	7.0
520	7697	-187	-176	-166	-200	-19	1.2	38	299	195	44.1
560	7839	-205	-195	-165	-211	-25	1.0	100	381	93	61.0

580	7910	-163	-176	-164	-172	-22	1.0	112	462	89	0.3
595	7963	-217	-211	-197	-224	-23	5.3	163	297	241	4.6
620	8052	-205	-201	-186	-210	-25	4.5	161	279	139	35.8
640	8123	-178	-174	-171	-191	-18	8.1	112	240	693	68.2

2. Adi Kolan (AKIII)

0	0	-127	-131	-121	-145	-15	0.4	58	614	1839	15.4
50	298	-125	-130	-121	-146	-13	1.3	80	468	1872	1.7
100	759	-127	-138	-123	-148	-13	0.7	41	590	1471	0.5
120	1024	-135	-140	-125	-156	-13	0.7	43	541	1799	3.1
130	1157	n.a.	n.a.	n.a.	n.a.	-14	0.7	41	495	1761	0.4
150	1422	-132	-138	-127	-152	-14	0.7	33	619	1466	3.2
170	1687	-123	-135	-124	-143	-13	0.7	30	554	1567	0.4
200	2084	-130	-134	-131	-150	-13	0.5	21	579	1258	1.8
210	2217	-140	-147	-153	-159	-15	0.6	n.a.	n.a.	n.a.	n.a.
220	2349	-126	-129	-125	-145	-14	0.8	15	584	1289	0.6
250	2377	-132	-117	-129	-153	-13	0.8	10	483	1280	14.0
270	2396	-134	-124	-125	-155	-13	0.9	10	361	1251	1.2
300	2424	-131	-122	-113	-151	-13	1.4	7	292	1740	14.8
310	2460	-125	-131	-121	-146	-13	2.2	10	265	1735	33.5
330	2586	-126	-133	-139	-146	-14	2.0	n.a.	n.a.	n.a.	n.a.
350	2711	-129	-123	-115	-150	-13	1.8	3	272	1880	32.6
360	2774	-146	-153	-159	-167	-12	1.8	n.a.	n.a.	n.a.	n.a.
370	2837	-136	-135	-124	-157	-13	1.6	4	286	1712	28.9
400	3025	-138	-148	-137	-159	-12	1.2	4	300	1135	22.8
420	3150	-137	-148	-140	-157	-13	1.3	3	283	1133	50.0
460	3401	-121	-145	-120	-141	-14	0.7	9	363	1235	26.1
480	3527	-110	-127	-112	-128	-15	0.3	0	721	1637	1.4
500	3652	-116	-116	-110	-135	-15	0.2	0	741	1832	3.3

520	3778	-145	-129	-121	-163	-15	0.3	0	330	1611	0.6
540	3903	-145	-135	-124	-164	-15	0.6	9	328	1933	7.9
580	4154	-142	-143	-131	-159	-16	0.1	0	559	1413	0.7
610	4342	-140	-142	-139	-159	-15	0.2	0	476	1976	20.9
620	13742	n.a.	n.a.	n.a.	n.a.	-17	0.1	0	558	1922	16.1
640	13742	-172	-129	-135	-185	-16	0.2	0	436	1964	13.5
3. Adigrat (ATI)											
0	485	-136	-142	-148	-149	-18	1.5	104	375	974	7.1
30	726	-127	-134	-140	-140	-19	1.2	n.a.	n.a.	n.a.	n.a.
70	1046	-134	-141	-147	-146	-20	0.9	52	464	859	7.6
100	1287	n.a.	n.a.	n.a.	n.a.	-19	0.9	50	475	835	6.4
120	1447	-137	-144	-150	-151	-19	1.0	47	458	824	4.4
150	1688	-144	-150	-157	-157	-19	0.9	49	475	821	5.4
170	1848	-136	-143	-149	-150	-18	0.9	45	464	844	1.0
200	2089	-150	-157	-163	-164	-19	1.1	44	421	991	13.8
230	2225	-133	-139	-145	-148	-17	0.9	n.a.	n.a.	n.a.	n.a.
260	2310	-135	-141	-147	-152	-16	0.4	34	481	935	1.1
300	2422	-135	-142	-148	-151	-17	0.4	32	597	757	0.9
320	2479	-153	-159	-166	-167	-18	0.3	32	731	778	1.0
350	2563	-139	-146	-152	-154	-18	0.4	n.a.	n.a.	n.a.	n.a.
380	2624	-135	-155	-161	-150	-18	0.3	n.a.	n.a.	n.a.	n.a.
430	2707	-149	-142	-148	-162	-19	0.2	14	875	771	1.9
460	2756	-129	-136	-142	-142	-19	0.2	n.a.	n.a.	n.a.	n.a.
500	2823	n.a.	n.a.	n.a.	n.a.	-15	0.1	n.a.	n.a.	1034	7.1
*510	2839	*-59	-66	-72	n.a.	-16	0.1	0	849	n.a.	n.a.
*530	2872	*-107	-114	-120	n.a.	-16	0.0	n.a.	n.a.	n.a.	n.a.

[a]From Gebru et al. (2009) and Terwilliger et al. (2011)

TOC = total organic carbon

C_3 corr = *n*-C_{26} corrected for D-enrichment from C_4 grasses The oldest of these estimates (ca. 14750 cal y BP) also has +5 ‰ added as a correction for different ice volume (see text).

HI, OI = hydrogen index, oxygen index from Rock-Eval pyrolysis

P = phosphorus

Char = charred organic matter

Table 3. Sequential linear trends in $\delta D_{n\text{-}C26}$ and bulk organic $\delta^{13}C$ values (Y) with age (X).

Y	Curve type	Breakpt (cal y BP)	Change (from older to younger)			
			All	Oldest to Breakpt	At Breakpt	Breakpt to youngest
1. Mai Maikden (MMII)						
$\delta D_{n\text{-}C26}$	5	6035			+	
$\delta^{13}C$ bulk m	5	6035			+	
$\delta^{13}C$ bulk t	6	6115		-	+	+
2. Adi Kolan (AKIII)						
$\delta D_{n\text{-}C26}$	1		+			
$\delta^{13}C$ bulk m	5	3435			+	
$\delta^{13}C$ bulk t	6	3435		+	+	-
3. Adigrat (ATI)						
$\delta D_{n\text{-}C26}$	6	2440		-	+	+
$\delta^{13}C$ bulk m	5	2110			-	
$\delta^{13}C$ bulk t	6	2680		-	+	-

m = only values corresponding to $\delta D_{n\text{-}C26}$ sample set.
t = all values.
+ = δ values increase significantly from older to younger sample ages.
- = δ values decrease significantly from older to younger sample ages.
Significance established at $p \leq 0.05$.

Curve types for relationship of δ (Y) to age (X)
0. no relationship, slope not significantly different from 0.
1. simple linear slope.
2. two sloping lines connected at a breakpt (breakpoint).
3. sloping line from maximum age to a breakpt, followed by no relationship to most recent age.
4. no relationship from maximum age to a breakpt, followed by sloping line to most recent age.
5. two disconnected intervals with slopes not significantly different from 0 but separated at a breakpt (ages older than breakpt ≠ younger ages)
6. two disconnected sloping lines separated at a breakpt.

Table 4. Correlations of soil micromorphological and chemical characteristics to one another and to δ values.

	Total P	%Char	%TOC	HI	OI	$\delta D_{n\text{-}C26}$
1. MMII						
%Char	n.s.					
%TOC	n.s.	n.s.				
HI	n.s.	n.s.	0.0005			
OI	n.s.	n.s.	-0.0070	-0.0010		
$\delta D_{n\text{-}C26}$	n.s.	n.s.	-0.0030	n.s.	0.014	
$\delta^{13}C$ bulk	n.s.	n.s.	n.s.	-0.0070	n.s.	0.040
2. AKIII						
%Char	n.s.					
%TOC	n.s.	0.0040				
HI	n.s.	n.s.	n.s.			
OI	n.s.	-0.0005	-0.0005	n.s.		
$\delta D_{n\text{-}C26}$	n.s.	n.s.	n.s.	n.s.	n.s.	
$\delta^{13}C$ bulk	-0.0500	n.s.	0.0005	n.s.	n.s.	n.s.
3. ATI						
%Char	0.0250					
%TOC	n.s.	n.s.				
HI	n.s.	n.s.	0.0005			
OI	n.s.	n.s.	-0.0020	-0.0020		
$\delta D_{n\text{-}C26}$	n.s.	n.s.	n.s.	n.s.	n.s.	
$\delta^{13}C$ bulk	n.s.	n.s.	n.s.	n.s.	n.s.	n.s.

Total P = Total Phosphorus (mg P kg^{-1} soil)
%Char = charred organic matter (% area)
%TOC = % Total organic carbon by weight
HI = Hydrogen Index (mg HC g^{-1} TOC)
OI = Oxygen Index mg O_2 g^{-1} TOC
numbers = maximum *p* values of significant correlations where negative values denote negative correlations
n.s. = not significant ($p > 0.05$)

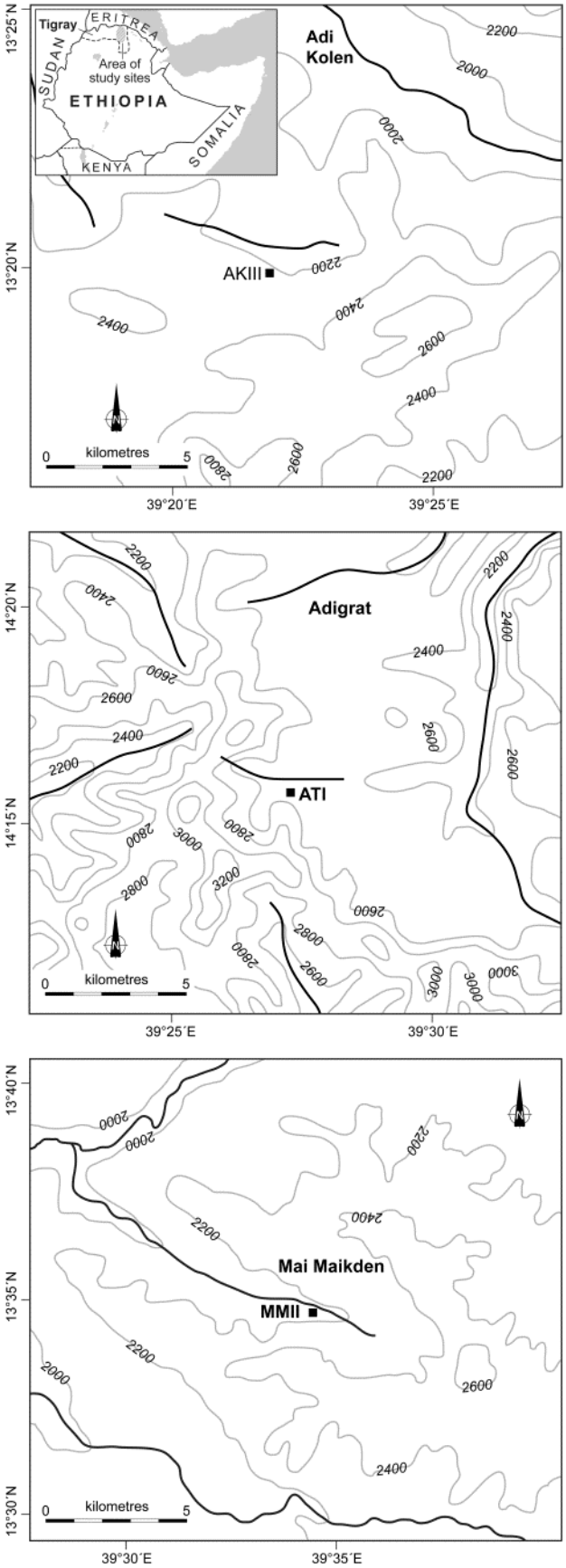
Tigray
ERITREA
SUDAN
Area of study sites
ETHIOPIA
SOMALIA
KENYA
Adi Kolen
AKIII
Adigrat
ATI
Mai Maikden
MMII
kilometres
0
5
13°25´N
13°20´N
14°20´N
14°15´N
13°40´N
13°35´N
13°30´N
39°20´E
39°25´E
39°30´E
39°35´E

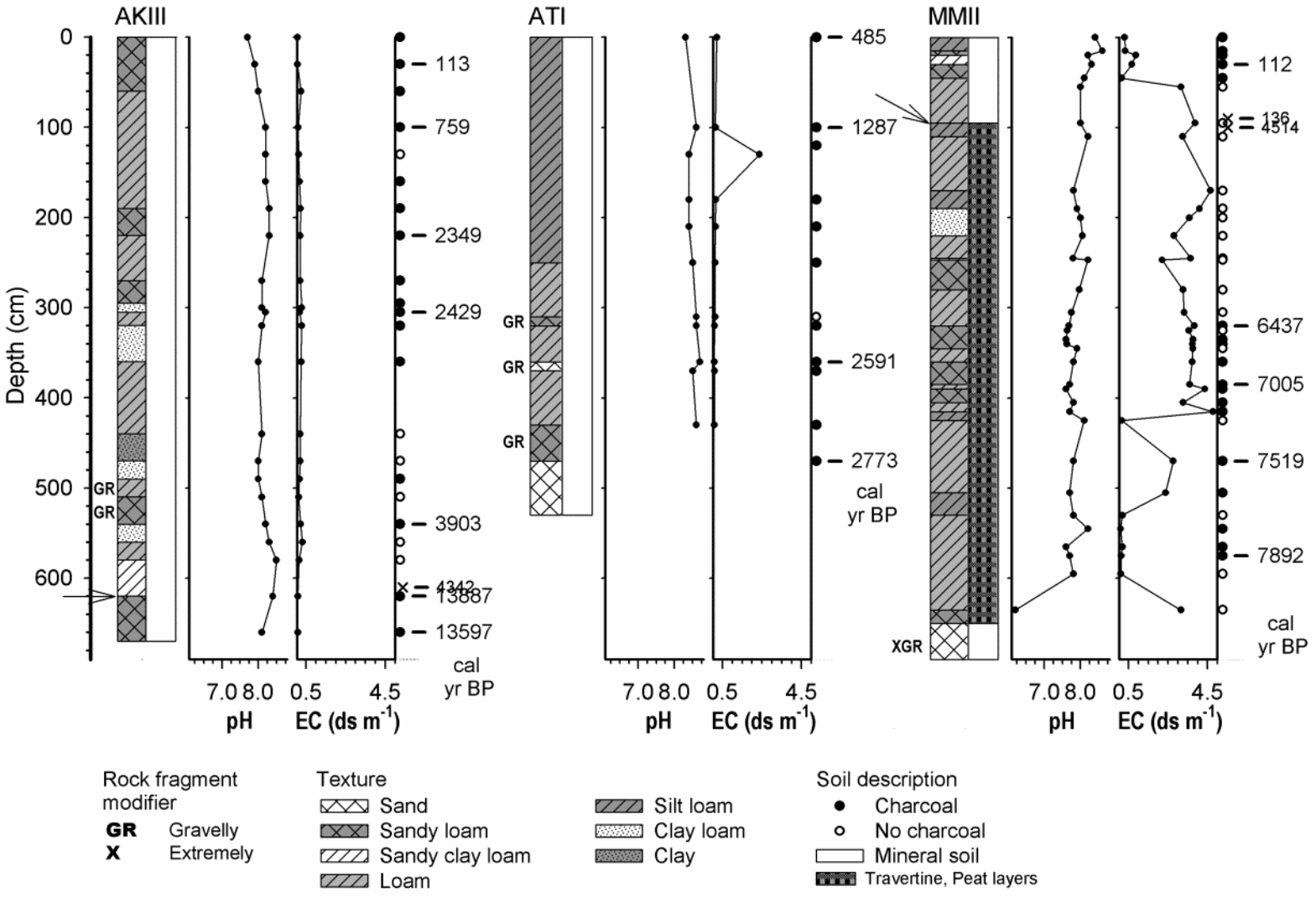
AKIII
ATI
MMII
Depth (cm)
0
100
200
300
400
500
600
GR
GR
GR
GR
XGR
113
759
2349
2429
3903
4342
13887
13597
485
1287
2591
2773
cal yr BP
112
136
4514
6437
7005
7519
7892
cal yr BP
7.0 8.0
pH
0.5 4.5
EC (ds m-1)
Rock fragment modifier
GR Gravelly
X Extremely
Texture
Sand
Sandy loam
Sandy clay loam
Loam
Silt loam
Clay loam
Clay
Soil description
Charcoal
No charcoal
Mineral soil
Travertine, Peat layers

Fig. 2

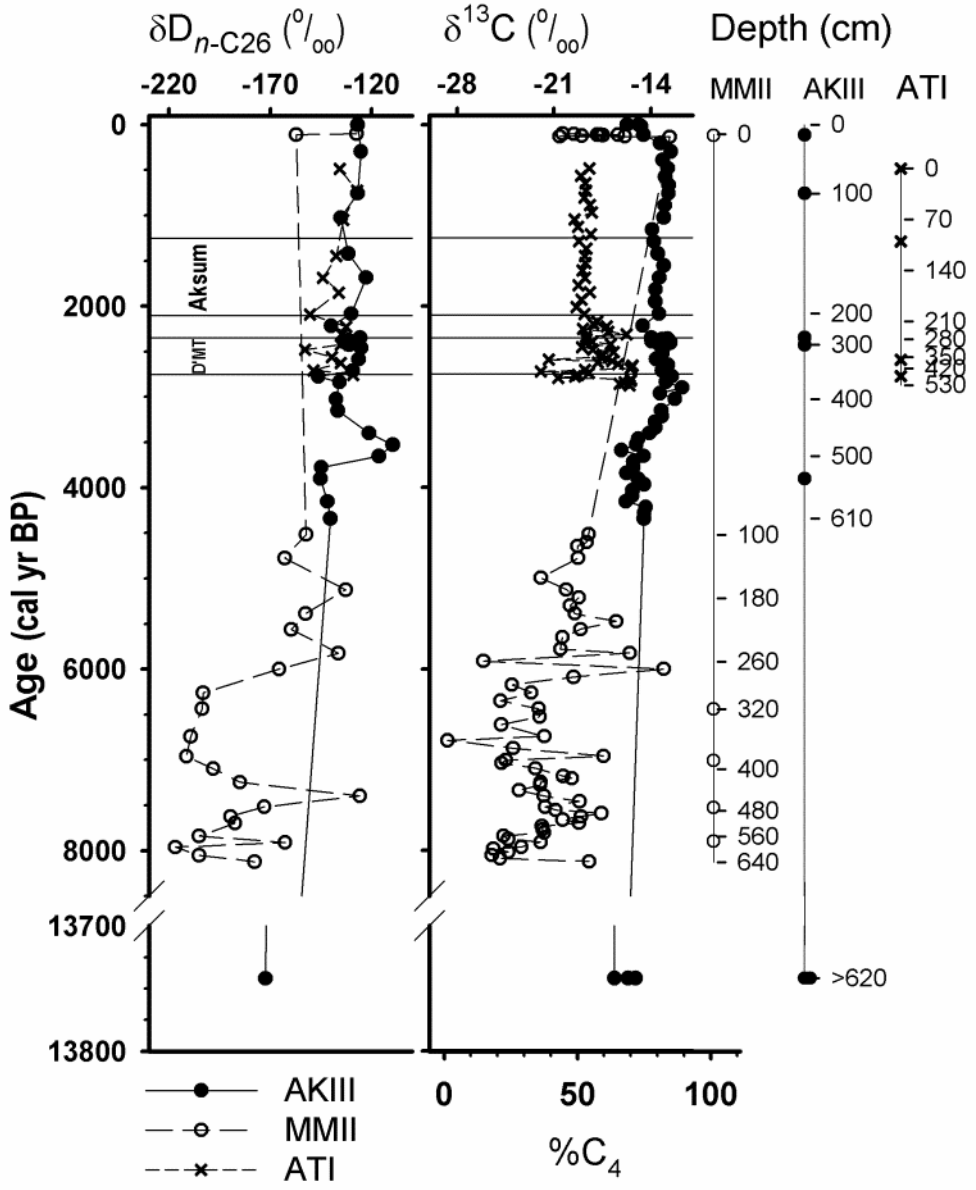
δD n-C26 (‰)
δ13C (‰)
Depth (cm)
-220
-170
-120
-28
-21
-14
MMII
AKIII
ATI
0
2000
4000
6000
8000
13700
13800
Age (cal yr BP)
Aksum
D'MIT
0
100
200
300
400
500
610
70
140
210
280
350
420
530
180
260
320
400
480
560
640
>620
AKIII
MMII
ATI
0
50
100
%C4

Fig. 3

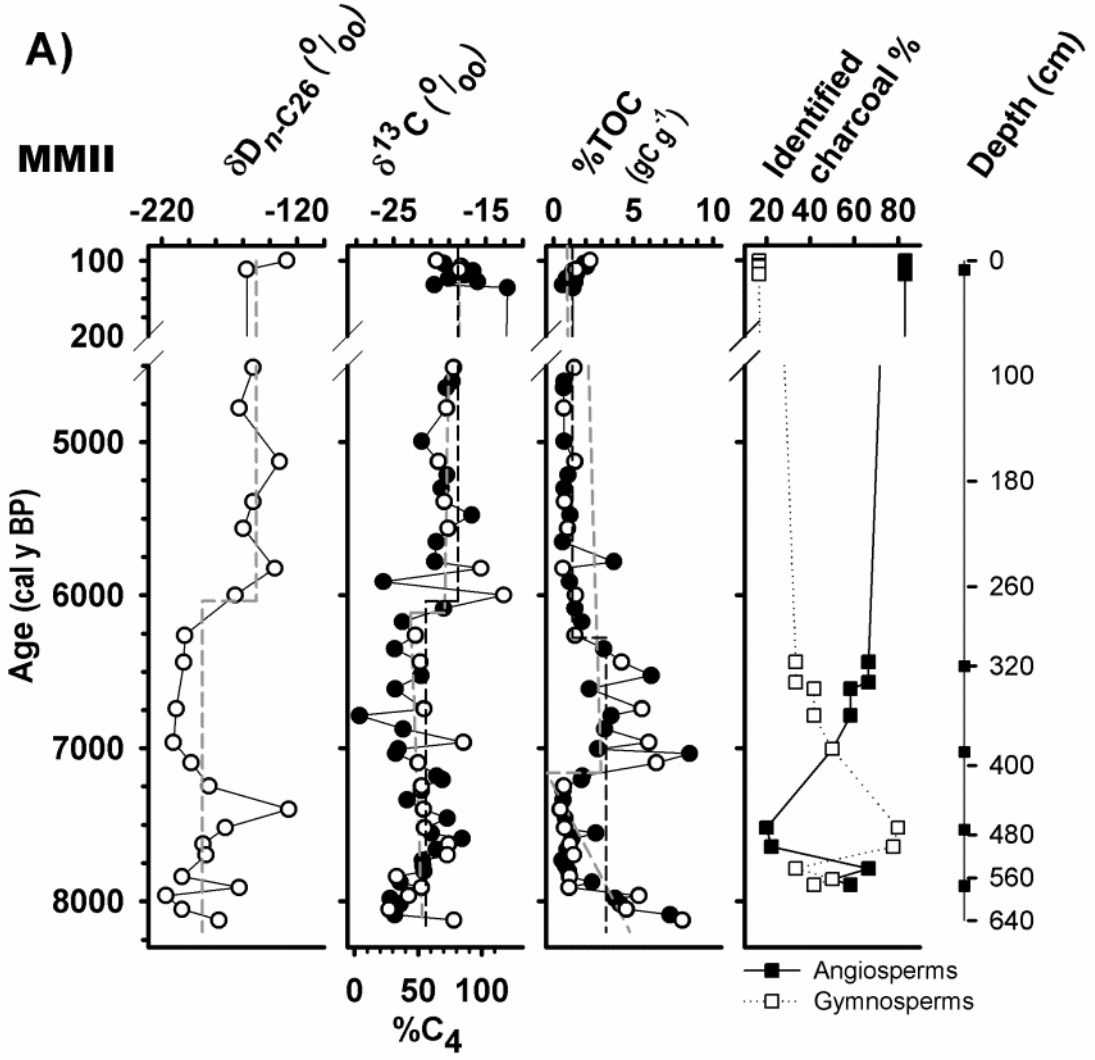
A)
MMII
δD n-C26 (‰)
δ13C (‰)
%TOC (gC g-1)
Identified charcoal %
Depth (cm)
-220
-120
-25
-15
0
5
10
20 40 60 80
100
200
5000
6000
7000
8000
Age (cal y BP)
0
100
180
260
320
400
480
560
640
0 50 100
%C4
Angiosperms
Gymnosperms

Fig. 4A

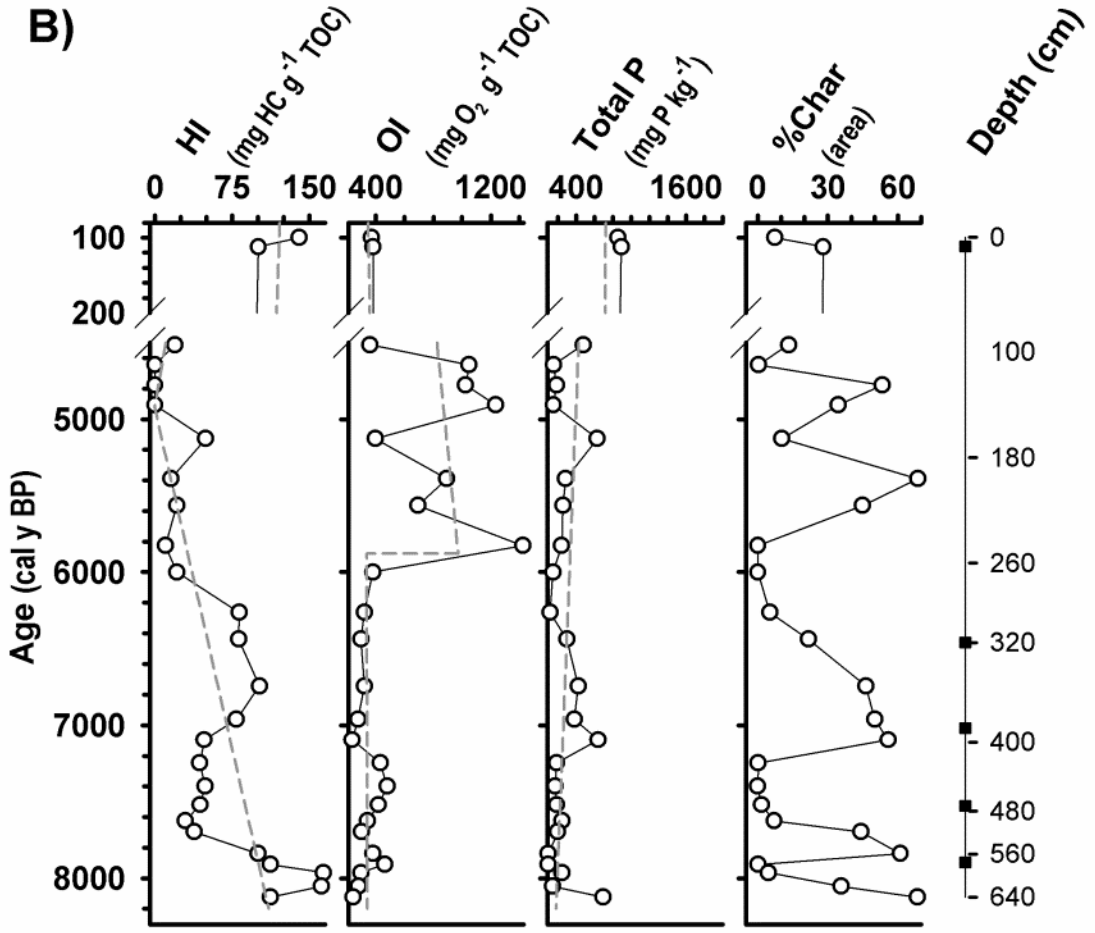
B)
HI
(mg HC g-1 TOC)
OI
(mg O2 g-1 TOC)
Total P
(mg P kg-1)
%Char
(area)
Depth (cm)
0 75 150
400 1200
400 1600
0 30 60
100
200
5000
6000
7000
8000
Age (cal y BP)
0
100
180
260
320
400
480
560
640

Fig. 4B

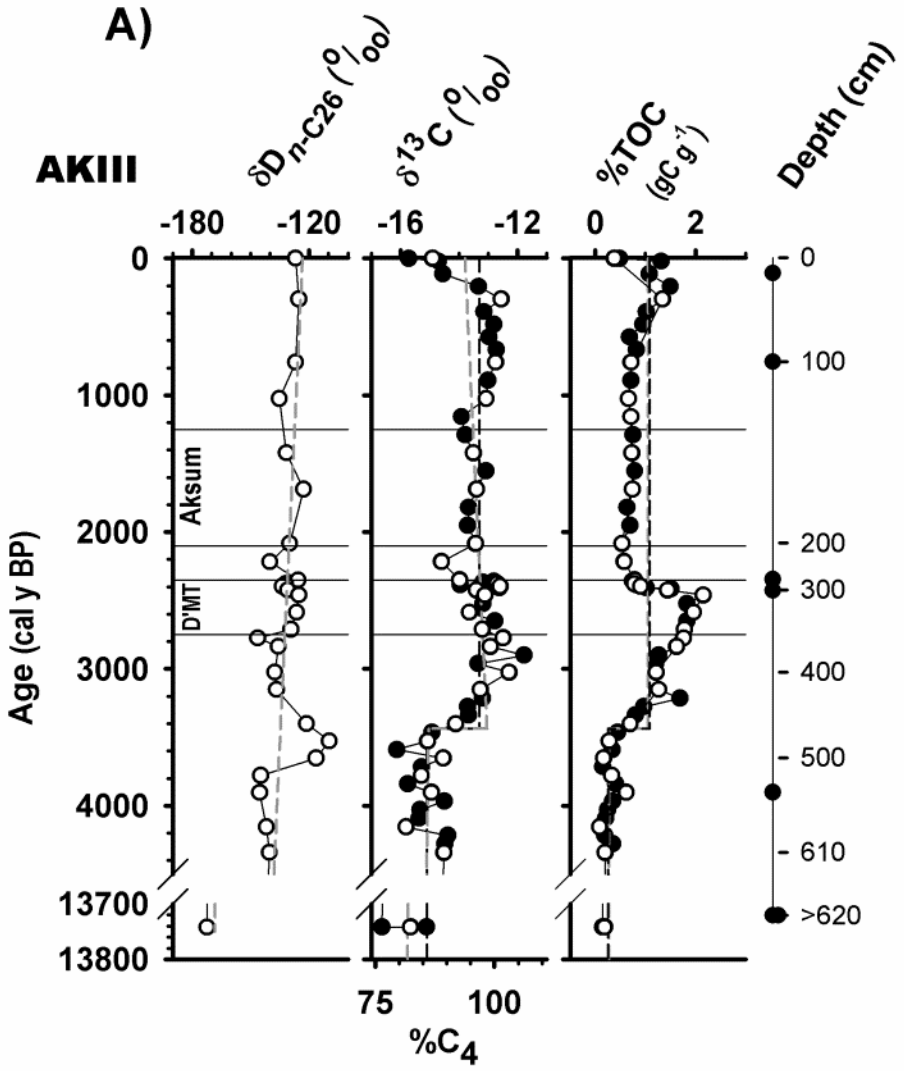
A)
AKIII
δD n-C26 (‰)
δ13C (‰)
%TOC
(gC g-1)
Depth (cm)
-180
-120
-16
-12
0
2
0
1000
2000
3000
4000
13700
13800
Aksum
D'MT
Age (cal y BP)
0
100
200
300
400
500
610
>620
75
100
%C4

Fig. 5A

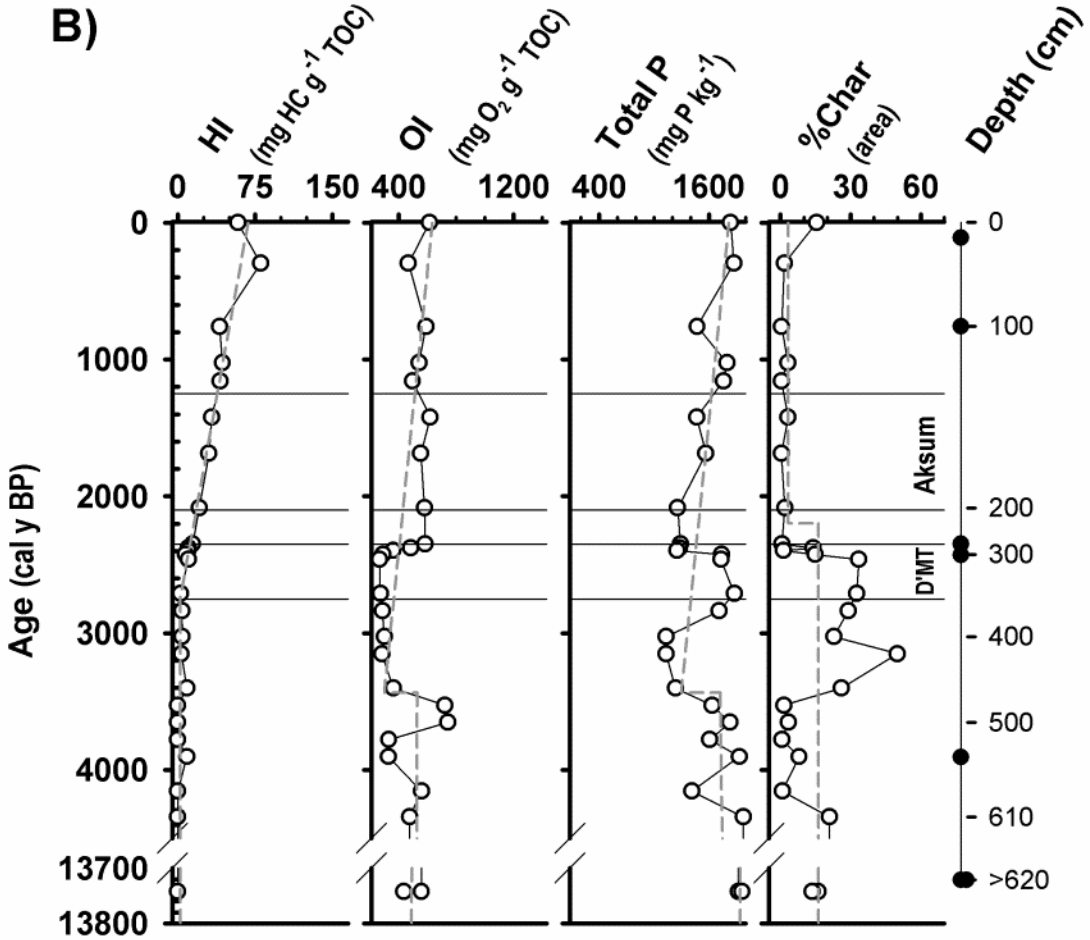
B)
HI
(mg HC g-1 TOC)
OI
(mg O2 g-1 TOC)
Total P
(mg P kg-1)
%Char
(area)
Depth (cm)
0
75
150
400
1200
400
1600
0
30
60
Age (cal y BP)
0
1000
2000
3000
4000
13700
13800
0
100
200
300
400
500
610
>620
Aksum
D'MT

Fig. 5B

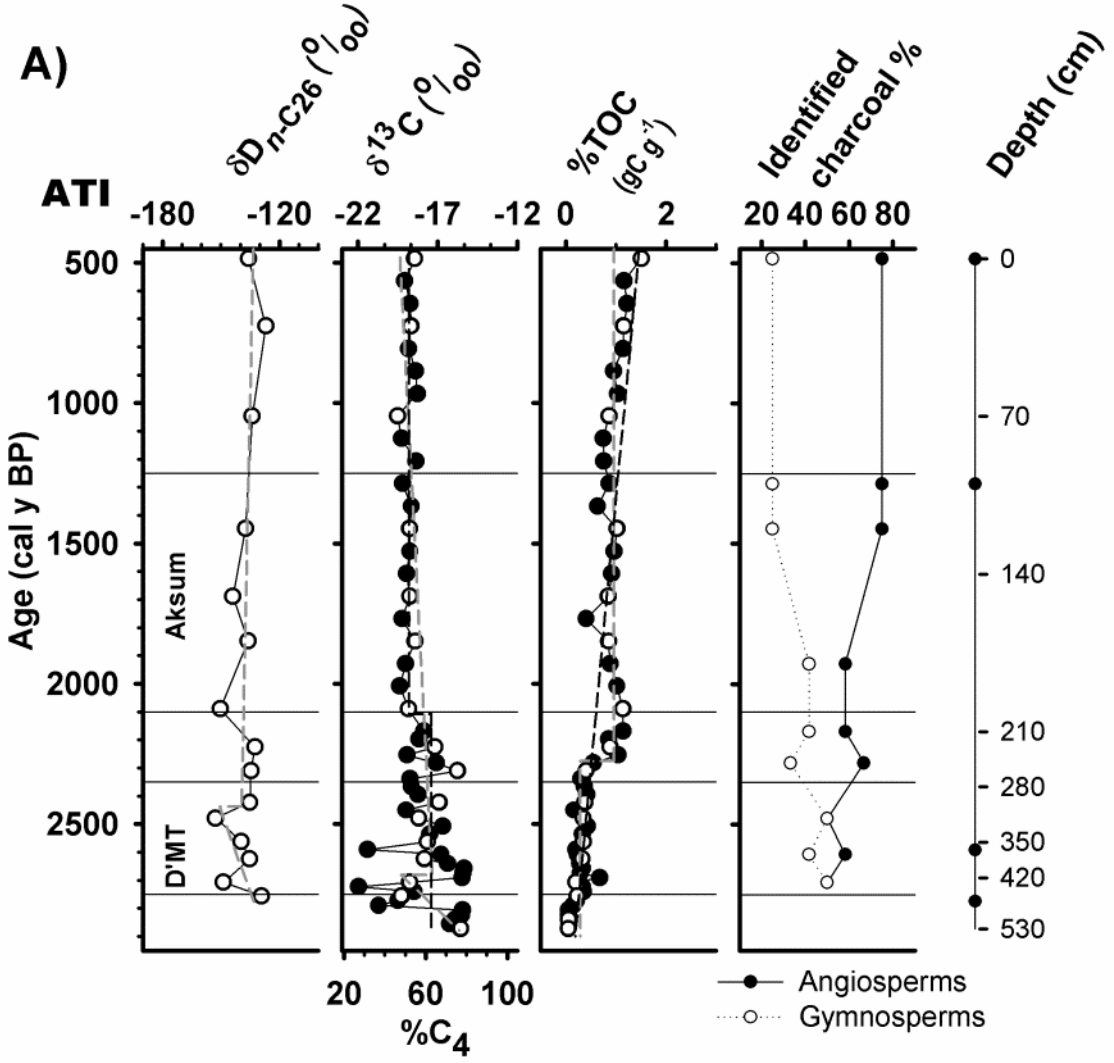
A)
ATI
δD n-C26 (‰)
δ13C (‰)
%TOC (gC g-1)
Identified charcoal %
Depth (cm)
-180
-120
-22
-17
-12
0
2
20 40 60 80
500
1000
1500
2000
2500
Age (cal y BP)
Aksum
D'MT
0
70
140
210
280
350
420
530
20
60
100
%C4
Angiosperms
Gymnosperms

Fig.6A

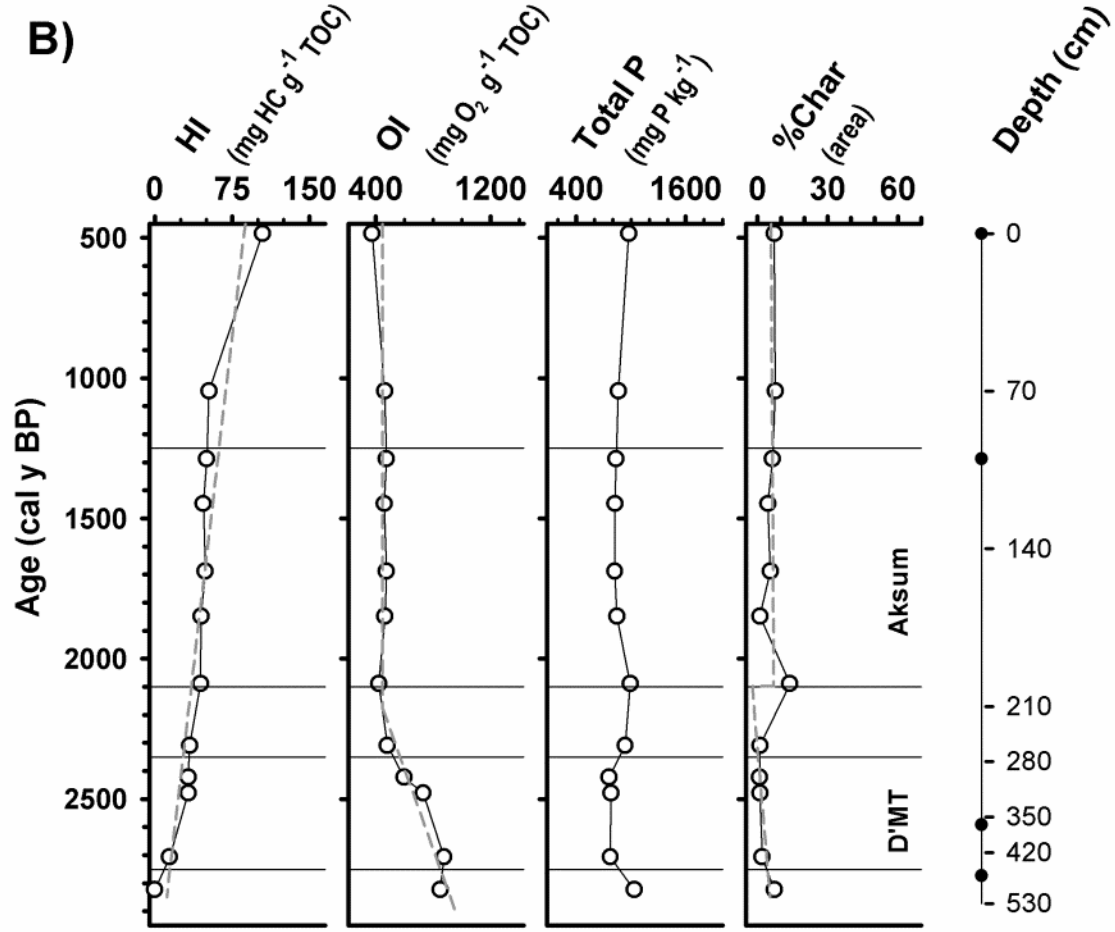
B)
HI
(mg HC g-1 TOC)
OI
(mg O2 g-1 TOC)
Total P
(mg P kg-1)
%Char
(area)
Depth (cm)
0
75
150
400
1200
400
1600
0
30
60
500
1000
1500
2000
2500
Age (cal y BP)
Aksum
D'MT
0
70
140
210
280
350
420
530

Fig. 6B